



Nonlinear thermal vibration of carbon nanotube polymer composite elliptical cylindrical shells

Ngo Dinh Dat · Tran Quoc Quan  · Nguyen Dinh Duc

Received: 17 February 2019 / Accepted: 21 May 2019 / Published online: 25 May 2019
© Springer Nature B.V. 2019

Abstract This paper investigated the nonlinear vibration and dynamic response of the carbon nanotube polymer composite elliptical cylindrical shells on elastic foundations in thermal environment. The material properties of the nanocomposite elliptical cylindrical shells are assumed to depend on temperature and graded in the thickness direction according to various linear functions. The shell is subjected to the combination of the uniformly distributed transverse load in harmonic form and the uniform temperature rise. The motion and geometrical compatibility equations are derived based on the Reddy's higher order shear deformation shell theory. The natural frequencies and the deflection amplitude–time curves of the shell are determined by using the Galerkin method and fourth-order Runge–Kutta method. The numerical results show not only the positive influences of carbon

nanotube volume fraction and elastic foundations but also the negative influences of initial imperfection and temperature increment on the nonlinear vibration and dynamic response of the carbon nanotube polymer composite elliptical cylindrical shells. The reliability of the present results is verified by comparing with other publications.

Keywords Nonlinear thermal vibration · The carbon nanotube polymer composite elliptical cylindrical shells · The Reddy's higher order shear deformation shell theory · Elastic foundations

1 Introduction

Nowadays, nanotechnology plays an important role in numerous industrial, commercial and engineering applications such as health, transportation, energy, environment, and many others. Because of unique features of mechanical strength, electrical and thermal conductivity, carbon nanotubes are chosen to be reinforcement in composite structures. Recently, carbon nanotube reinforced composites have been properly noticed. Arani et al. (2014) conducted the static stress analysis of carbon nanotube reinforced composite cylinder subjected to non-axisymmetric thermo-mechanical loads and uniform electro-magnetic fields. Shen (2009) presented an research on the

N. D. Dat
NTT Institute of High Technology, Nguyen Tat Thanh
University, Ho Chi Minh City, Vietnam

T. Q. Quan (✉) · N. D. Duc
Advanced Materials and Structures Laboratory, VNU –
Hanoi – University of Engineering and Technology
(UET), 144 Xuan Thuy, Cau Giay, Hanoi, Vietnam
e-mail: quantq1505@gmail.com

N. D. Duc
National Research Laboratory, Department of Civil and
Environmental Engineering, Sejong University,
209 Neungdong-ro, Gwangjin-gu, Seoul 05006,
Republic of Korea

nonlinear thermal bending of functionally graded single-walled carbon nanotube reinforced nanocomposite plates under a transverse uniform or sinusoidal load with simply supported edges. Based on the first order shear deformation theory, Lei et al. (2016) studied stability of functionally graded composites laminated plate reinforced by carbon nanotubes. Mirzaei and Kiani (2016) dealt with thermal buckling of functionally graded carbon nanotube reinforced conical shell. Zarei et al. (2017) evaluated multiple impact response of composite plates reinforced by carbon nanotube with general boundary conditions in case of temperature dependent properties. Kundalwal and Meguid (2015) studied the effect of carbon nanotube waviness on the active constrained layer damping of the laminated hybrid composite shells; Kundalwal and Ray (2016) also introduced the investigation of active constrained layer damping of smart laminated fuzzy fiber reinforced composite plates. Shen and Xiang (2012) investigated the nonlinear vibration of nanotube composite cylindrical shells reinforced by single-walled carbon nanotubes under a uniform temperature rise; Alibeigloo (2014) carried out the free vibration analysis of composite cylindrical panel with a polymeric matrix and carbon nanotube fibers embedded in piezoelectric layers based on theory of elasticity. A new approach—using analytical solution to investigate nonlinear dynamic response and vibration of imperfect functionally graded carbon nanotube reinforced composite double curved shallow shells was introduced in (Duc et al. 2017). Baloch et al. (2018) presented residual mechanical properties of lightweight concrete and normal strength concrete containing multi-walled carbon nanotubes after exposure to high temperatures. Kumar et al. (2017) concerned with the analysis of active constrained layer damping of geometrically nonlinear vibrations of doubly curved sandwich shells with facings composed of fuzzy fiber reinforced composite. Based on generalized differential quadrature method, Keleshteri et al. (2017) investigated stability of smart functionally graded carbon nanotube reinforced composites annular sector plates with surface-bonded piezoelectric layers. Further, Asadi and Wang (2017) examined dynamic stability of a pressurized functionally graded carbon nanotube reinforced composites cylindrical shell interacting with supersonic airflow.

In order to investigate the mechanical properties of thick structures, the higher order shear deformation

plate and shell theories must be used because the Kirchoff hypothesis is not true in this case. Although the calculations of the higher order shear deformation plate and shell theories are much more complex than ones of the classical or the first order shear deformation plate and shell theories, there are still many publications on static and dynamic stability of structures using these theories. The dynamic instability behavior of laminated hyper and conoid shells using a higher order shear deformation theory were researched in (Pradyumna and Bandyopadhyay 2011). Dastjerdi et al. (2017) studied and solved the nonlinear local and nonlocal analysis of an annular sector plate based on a new modified higher-order shear deformation theory. Phung-Van et al. (2015) presented a simple and effective formulation based on isogeometric analysis and higher order shear deformation theory to investigate static, free vibration and dynamic control of piezoelectric composite plates integrated with sensors and actuators. Xie et al. (2019) proposed a general higher-order shear deformation zig-zag theory for predicting the nonlinear aerothermoelastic characteristics of composite laminated panels subjected to supersonic airflow. Chen et al. (2018) considered thermal vibration of beams made of FGM with general boundary conditions using third order shear deformation beam theory. Mantari et al. (2012) focused on bending and free vibration analysis of isotropic and multilayered plates and shells. Further, Tu et al. (2010) developed a nine-noded rectangular element with nine degrees of freedom at each node for the bending and vibration analysis of laminated and sandwich composite plates. Duc et al. (2015) investigated the nonlinear vibration and dynamic analysis of imperfect thick functionally graded double curved shallow shells with piezoelectric actuators on elastic foundations subjected to the combination of electrical, thermal, mechanical and damping loading. Jadhav and Bajoria (2015) presented the buckling of functionally graded plate integrated with piezoelectric actuator and sensor at the top and bottom faces subjected to the combination of electrical and mechanical loading.

The elliptical cylindrical shell is one of the special shapes of the cylindrical shell. Because these structures are used extensively in various fields such as aerospace, marine, pipelines, missiles and automobiles engineering; they attracted great attention of the scientist around the world. Free and forced vibration

characteristics of submerged finite elliptic cylindrical shell were conducted in (Zhang et al. 2017). Ganapathi et al. (2004) considered the free flexural vibration behavior of laminated angle-ply elliptical cylindrical shells. Kazemi et al. (2012) focused on the stability analysis of piezoelectric elliptical cylindrical shell using finite element method based on the shear deformation theory. Khalifa (2015) evaluated effects of non-uniform Winkler foundation and non-homogeneity on the free vibration of an orthotropic elliptical cylindrical shell. Li et al. (2014) investigated the elastic critical load of submerged elliptical cylindrical shell based on the vibro-acoustics model. Up to date, there are very few publications about elliptical cylindrical shells using higher order shear deformation theory. Duc et al. (2016) analyzed nonlinear thermal stability of FGM elliptical cylindrical shells reinforced by eccentrically stiffened. Ahmed (2016) considered the effects of the crease parameters and the elastic foundation on the buckling behavior of isotropic and orthotropic elliptic cylindrical shells with cosine-shaped meridian under radial loads. Recently, Xu et al. (2017) introduced a recent computational study to obtain the nonlinear buckling resistance of perfect elastic circular cylindrical shells subjected to uniform bending.

This paper introduces an analytical approach on the nonlinear dynamic response and vibration of carbon nanotube polymer composite elliptical cylindrical shells on elastic foundations in the thermal environment using the Reddy’s higher order shear deformation shell theory. The material properties of the shell are supposed to depend on temperature. The natural frequencies and deflection–time relationship are obtained by Galerkin method and fourth-order Runge–Kutta method. The numerical results show the effects of geometrical properties, temperature increment, initial imperfection, elastic foundations, volume fraction of carbon nanotube of the nonlinear dynamic response and vibration of the carbon nanotube polymer composite elliptical cylindrical shells.

2 Problem formulation

Consider a carbon nanotube polymer composite elliptical cylindrical shells as Fig. 1. The length, mean radius and total thickness of the shell are L, R and h , respectively. A coordinate system (x, θ, z) is defined

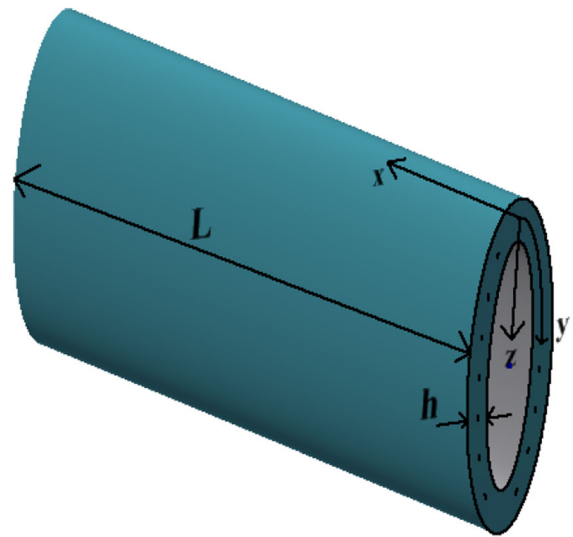


Fig. 1 Geometry and the coordinate system of the carbon nanotube polymer composite elliptical cylindrical shells

in which θ and x are in the circumferential and axial directions of the shell, respectively, and z is perpendicular to the surface and points outwards ($-h/2 \leq z \leq h/2$).

The carbon nanotube polymer composite elliptical cylindrical shells are assumed to surround on elastic foundations as Fig. 2. The interaction between the elastic foundations and the shells is described by Pasternak model as (Duc et al. 2015, 2016)

$$q_e = k_1 w - k_2 \left(\frac{\partial^2 w}{\partial x^2} + \frac{\partial^2 w}{\partial y^2} \right), \tag{1}$$

where w is the deflection of the carbon nanotube polymer composite elliptical cylindrical shells; k_1 and k_2 are stiffness of Winkler and Pasternak foundation, respectively.

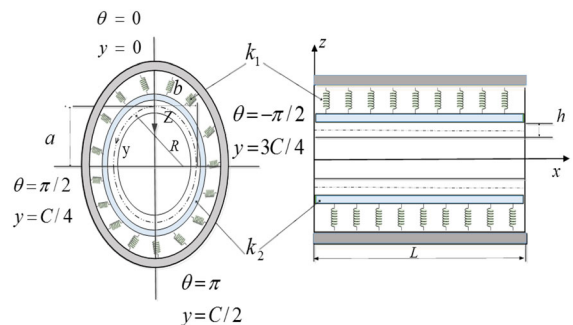


Fig. 2 Model of the carbon nanotube polymer composite elliptical cylindrical shells on elastic foundations

The principal radii of curvature in the circumferential direction R can be determined to the minor radius b and the major radius a of elliptical cross-section as (Duc et al. 2016; Xu et al. 2017)

$$R = (b^2/R_0)(1 + \mu_0 \cos 2\theta)^{-3/2}, \quad (2)$$

with

$$R_0 = \sqrt{(a^2 + b^2)/2}, \quad \mu_0 = a^2 - b^2/(a^2 + b^2), \quad (3)$$

3 The elastic moduli and the thermal expansion coefficients of the carbon nanotube polymer composite

3.1 Elastic moduli

It is assumed that the carbon nanotube polymer composite material is made from Poly (methyl methacrylate), referred to as PMMA, reinforced by (10,10) single-walled carbon nanotubes. The effective Young's and shear modulus of the carbon nanotube polymer composite material are determined as (Shen 2009; Mirzaei and Kiani 2016)

$$\begin{aligned} E_{11} &= \eta_1 V_{CNT} E_{11}^{CNT} + V_m E_m, \\ \frac{\eta_2}{E_{22}} &= \frac{V_{CNT}}{E_{22}^{CNT}} + \frac{V_m}{E_m}, \\ \frac{\eta_3}{G_{12}} &= \frac{V_{CNT}}{G_{12}^{CNT}} + \frac{V_m}{G_m}, \end{aligned} \quad (4)$$

where V_{CNT} and V_m are the volume fractions of the carbon nanotubes and the polymer matrix, respectively; E_{11}^{CNT} , E_{22}^{CNT} , G_{12}^{CNT} are the mechanical properties of the carbon nanotubes; E_m , G_m are Young's and shear moduli of the polymer matrix and η_i ($i = \overline{1, 3}$) are the carbon nanotubes efficiency parameters.

The volume fractions of the carbon nanotubes and the polymer matrix are assumed to grade in the thickness direction according to linear functions. Three types of carbon nanotubes reinforcement, i.e. UD, V and X are considered with the volume fractions of the three distribution types are expressed as follows (Shen 2009; Mirzaei and Kiani 2016)

$$V_{CNT}(z) = \begin{cases} V_{VCT}^* & (UD) \\ V_{VCT}^* \left(1 + 2 \frac{z}{h}\right) & (V) \\ 4V_{VCT}^* \frac{|z|}{h} & (X) \end{cases}, \quad (5)$$

$$V_m(z) = 1 - V_{CNT}(z),$$

where

$$V_{CNT}^* = \frac{w_{CNT}}{w_{CNT} + (\rho_{CNT}/\rho_m) - (\rho_{CNT}/\rho_m)w_{CNT}}, \quad (6)$$

in which w_{CNT} is the mass fraction of carbon nanotubes, and ρ_{CNT} and ρ_m are the densities of carbon nanotubes and polymer matrix, respectively.

The elastic moduli (except the Poisson's ratio) of the polymer matrix are dependent to temperature as (Shen 2009; Shen and Xiang 2012)

$$\begin{aligned} E_m &= (3.52 - 0.0034T) \text{ GPa}, \\ \nu_m &= 0.34, \\ \alpha_m &= 45(1 + 0.0005\Delta T) \times 10^{-6} / \text{K}, \end{aligned} \quad (7)$$

where $T = 300 + \Delta T$, ΔT is the change of temperature in the environment.

The value of Young's modulus, shear modulus and thermal expansion coefficient of (10,10) single-walled carbon nanotubes are assumed to depend on temperature and they are calculated at five values of temperature by molecular dynamics simulations in Table 1 (Mirzaei and Kiani 2016). The Poisson's ratio of single-walled carbon nanotubes is chosen to be constant $\nu_{12}^{CNT} = 0.175$.

Table 2 shows the values of the carbon nanotubes efficiency parameters η_i ($i = \overline{1, 3}$) at three values of nanotube volume fractions (Shen 2009; Mirzaei and Kiani 2016; Shen and Xiang 2012).

The effective Poisson's ratio of the carbon nanotube polymer composite material depends on the temperature and the thickness direction as (Shen 2009; Shen and Xiang 2012)

$$\nu_{12} = V_{CNT}^* \nu_{12}^{CNT} + V_m \nu_m, \quad (8)$$

where ν_{12}^{CNT} and ν_m are Poisson's ratio of the carbon nanotubes and the polymer matrix, respectively.

3.2 Thermal expansion coefficients

The thermal expansion coefficients of the carbon nanotube polymer composite material in the

Table 1 The material properties of (10, 10) single-walled carbon nanotubes at five values of temperature

T (K)	E_{22}^{CNT} (TPa)	E_{11}^{CNT} (TPa)	G_{12}^{CNT} (TPa)	α_{11}^{CNT} ($\times 10^{-6}/K$)	α_{22}^{CNT} ($\times 10^{-6}/K$)
300	7.0800	5.6466	1.9445	3.4584	5.1682
400	6.9814	5.5679	1.9703	4.1496	5.0905
500	6.9348	5.5308	1.9643	4.5361	5.0189
700	6.8641	5.4744	1.9644	4.6677	4.8943

Table 2 The values of the carbon nanotubes efficiency parameters at three values of nanotube volume fractions

V_{CNT}^*	η_1	η_2	η_3
0.12	0.137	1.022	0.715
0.17	0.141	1.626	1.138
0.28	0.141	1.585	1.109

longitudinal and transverse directions are expressed by (Shen 2009)

$$\alpha_{11} = \frac{V_{CNT}E_{11}^{CNT}\alpha_{11}^{CNT} + V_mE_m\alpha_m}{V_{CNT}E_{11}^{CNT} + V_mE_m},$$

$$\alpha_{22} = (1 + \nu_{12}^{CNT})V_{CNT}\alpha_{22}^{CNT} + (1 + \nu_m)V_m\alpha_m - \nu_{12}\alpha_{11}, \tag{9}$$

with α_m and $\alpha_{11}^{CNT}, \alpha_{22}^{CNT}$ are the thermal expansion coefficients of the polymer matrix and the carbon nanotubes, respectively.

4 Nonlinear strain–displacement relations

The nonlinear relations between strain and displacement of the carbon nanotube polymer composite elliptical cylindrical shells are (Brush and Almroth 1975; Reddy 2004)

$$\begin{pmatrix} \epsilon_x \\ \epsilon_y \\ \gamma_{xy} \end{pmatrix} = \begin{pmatrix} \epsilon_x^0 \\ \epsilon_y^0 \\ \gamma_{xy}^0 \end{pmatrix} + z \begin{pmatrix} k_x^1 \\ k_y^1 \\ k_{xy}^1 \end{pmatrix} + z^3 \begin{pmatrix} k_x^3 \\ k_y^3 \\ k_{xy}^3 \end{pmatrix}, \tag{10}$$

$$\begin{pmatrix} \gamma_{xz} \\ \gamma_{yz} \end{pmatrix} = \begin{pmatrix} \gamma_{xz}^0 \\ \gamma_{yz}^0 \end{pmatrix} + z^2 \begin{pmatrix} k_{xz}^2 \\ k_{yz}^2 \end{pmatrix},$$

where

$$\begin{pmatrix} \epsilon_x^0 \\ \epsilon_y^0 \\ \gamma_{xy}^0 \end{pmatrix} = \begin{pmatrix} \frac{\partial u}{\partial x} + \frac{1}{2} \left(\frac{\partial w}{\partial x} \right)^2 \\ \frac{\partial v}{\partial y} - \frac{w}{R} + \frac{1}{2} \left(\frac{\partial w}{\partial y} \right)^2 \\ \frac{\partial u}{\partial y} + \frac{\partial v}{\partial x} + \frac{\partial w}{\partial x} \frac{\partial w}{\partial y} \end{pmatrix},$$

$$\begin{pmatrix} k_x^1 \\ k_y^1 \\ k_{xy}^1 \end{pmatrix} = \begin{pmatrix} \frac{\partial \phi_x}{\partial x} \\ \frac{\partial \phi_y}{\partial y} \\ \frac{\partial \phi_x}{\partial y} + \frac{\partial \phi_y}{\partial x} \end{pmatrix}, \quad \begin{pmatrix} \gamma_{xz}^0 \\ \gamma_{yz}^0 \end{pmatrix} = \begin{pmatrix} \phi_x + \frac{\partial w}{\partial x} \\ \phi_y + \frac{\partial w}{\partial y} \end{pmatrix},$$

$$\begin{pmatrix} k_x^3 \\ k_y^3 \\ k_{xy}^3 \end{pmatrix} = -c_1 \begin{pmatrix} \frac{\partial \phi_x}{\partial x} + \frac{\partial^2 w}{\partial x^2} \\ \frac{\partial \phi_y}{\partial y} + \frac{\partial^2 w}{\partial y^2} \\ \frac{\partial \phi_x}{\partial y} + \frac{\partial \phi_y}{\partial x} + 2 \frac{\partial^2 w}{\partial x \partial y} \end{pmatrix},$$

$$\begin{pmatrix} k_{xz}^2 \\ k_{yz}^2 \end{pmatrix} = -3c_1 \begin{pmatrix} \phi_x + \frac{\partial w}{\partial x} \\ \phi_y + \frac{\partial w}{\partial y} \end{pmatrix}, \tag{11}$$

in which $c_1 = 4/3h^2$; ϕ_x, ϕ_y are the rotations of normals to the midsurface with respect to the y and x axes, respectively.

5 Hooke’s law

Hooke’s law for a carbon nanotube polymer composite elliptical cylindrical shells with temperature-dependent properties is defined as (Alibeigloo 2014)

$$\begin{bmatrix} \sigma_{xx} \\ \sigma_{yy} \\ \sigma_{xy} \\ \sigma_{xz} \\ \sigma_{yz} \end{bmatrix} = \begin{bmatrix} Q_{11} & Q_{12} & 0 & 0 & 0 \\ Q_{12} & Q_{22} & 0 & 0 & 0 \\ 0 & 0 & Q_{66} & 0 & 0 \\ 0 & 0 & 0 & Q_{44} & 0 \\ 0 & 0 & 0 & 0 & Q_{55} \end{bmatrix} \begin{bmatrix} \varepsilon_{xx} - \alpha_{11}\Delta T \\ \varepsilon_{yy} - \alpha_{22}\Delta T \\ \varepsilon_{xy} \\ \varepsilon_{xz} \\ \varepsilon_{yz} \end{bmatrix}, \tag{12}$$

where

$$\begin{aligned} Q_{11} &= \frac{E_{11}}{1 - \nu_{12}\nu_{21}}, & Q_{22} &= \frac{E_{22}}{1 - \nu_{12}\nu_{21}}, \\ Q_{12} &= \frac{\nu_{21}E_{11}}{1 - \nu_{12}\nu_{21}}, & Q_{44} &= G_{23}, & Q_{55} &= G_{13}, \\ Q_{66} &= G_{12}, \end{aligned} \tag{13}$$

and we assume that $G_{13} = G_{12}$ and $G_{23} = 1.2G_{12}$ (Shen and Xiang 2012).

6 Forces and moments

The force and moment resultants of the carbon nanotube polymer composite elliptical cylindrical shells are expressed by

$$\begin{aligned} (N_i, M_i, P_i) &= \int_{-h/2}^{h/2} \sigma_i(1, z, z^3) dz, & i &= x, y, xy \\ (Q_i, R_i) &= \int_{-h/2}^{h/2} \sigma_{iz}(1, z^2) dz, & i &= x, y. \end{aligned} \tag{14}$$

Substitution Eqs. (10) and (11) into Eqs. (12) then results into Eqs. (14) yields the constitutive relations as

in which

$$\begin{aligned} &(A_{ij}, B_{ij}, D_{ij}, E_{ij}, F_{ij}, H_{ij}) \\ &= \int_{-h/2}^{h/2} Q_{ij}(1, z, z^2, z^3, z^4, z^6) dz, & ij &= 11, 12, 22, 66, \\ &(A_{kl}, D_{kl}, F_{kl}) = \int_{-h/2}^{h/2} Q_{ij}(1, z^2, z^4) dz, & kl &= 44, 55, \\ \Phi_1 &= \int_{-h/2}^{h/2} Q_{11}\alpha_{11}\Delta T dz + \int_{-h/2}^{h/2} Q_{12}\alpha_{22}\Delta T dz, \\ \Phi_2 &= \int_{-h/2}^{h/2} Q_{12}\alpha_{11}\Delta T dz + \int_{-h/2}^{h/2} Q_{22}\alpha_{22}\Delta T dz, \\ \Phi_3 &= \int_{-h/2}^{h/2} Q_{11}\alpha_{11}\Delta T z dz + \int_{-h/2}^{h/2} Q_{12}\alpha_{22}\Delta T z dz, \\ \Phi_4 &= \int_{-h/2}^{h/2} Q_{12}\alpha_{11}\Delta T z dz + \int_{-h/2}^{h/2} Q_{22}\alpha_{22}\Delta T z dz, \\ \Phi_5 &= \int_{-h/2}^{h/2} Q_{11}\alpha_{11}\Delta T z^3 dz + \int_{-h/2}^{h/2} Q_{12}\alpha_{22}\Delta T z^3 dz, \\ \Phi_6 &= \int_{-h/2}^{h/2} Q_{12}\alpha_{11}z^3\Delta T dz + \int_{-h/2}^{h/2} Q_{22}\alpha_{22}z^3\Delta T dz, \end{aligned} \tag{16}$$

From the constitutive relations (15), we have

$$\begin{Bmatrix} N_x \\ N_y \\ N_{xy} \\ M_x \\ M_y \\ M_{xy} \\ P_x \\ P_y \\ P_{xy} \\ Q_x \\ Q_y \\ R_x \\ R_y \end{Bmatrix} = \begin{bmatrix} A_{11} & A_{12} & 0 & B_{11} & B_{12} & 0 & E_{11} & E_{12} & 0 & 0 & 0 & 0 & 0 \\ A_{12} & A_{22} & 0 & B_{12} & B_{22} & 0 & E_{12} & E_{22} & 0 & 0 & 0 & 0 & 0 \\ 0 & 0 & A_{66} & 0 & 0 & B_{66} & 0 & 0 & E_{66} & 0 & 0 & 0 & 0 \\ B_{11} & B_{12} & 0 & D_{11} & D_{12} & 0 & F_{11} & F_{12} & 0 & 0 & 0 & 0 & 0 \\ B_{12} & B_{22} & 0 & D_{12} & D_{22} & 0 & F_{12} & F_{22} & 0 & 0 & 0 & 0 & 0 \\ 0 & 0 & B_{66} & 0 & 0 & D_{66} & 0 & 0 & F_{66} & 0 & 0 & 0 & 0 \\ E_{11} & E_{12} & 0 & F_{11} & F_{12} & 0 & H_{11} & H_{12} & 0 & 0 & 0 & 0 & 0 \\ E_{12} & E_{22} & 0 & F_{12} & F_{22} & 0 & H_{12} & H_{22} & 0 & 0 & 0 & 0 & 0 \\ 0 & 0 & E_{66} & 0 & 0 & F_{66} & 0 & 0 & H_{66} & 0 & 0 & 0 & 0 \\ 0 & 0 & 0 & 0 & 0 & 0 & 0 & 0 & 0 & A_{44} & 0 & D_{44} & 0 \\ 0 & 0 & 0 & 0 & 0 & 0 & 0 & 0 & 0 & 0 & A_{55} & 0 & D_{55} \\ 0 & 0 & 0 & 0 & 0 & 0 & 0 & 0 & 0 & D_{44} & 0 & F_{44} & 0 \\ 0 & 0 & 0 & 0 & 0 & 0 & 0 & 0 & 0 & 0 & D_{55} & 0 & F_{55} \end{bmatrix} \begin{Bmatrix} \varepsilon_x^0 \\ \varepsilon_y^0 \\ \gamma_{xy}^0 \\ k_x^1 \\ k_y^1 \\ k_{xy}^1 \\ k_x^3 \\ k_y^3 \\ k_{xy}^3 \\ \gamma_{xz}^0 \\ \gamma_{yz}^0 \\ k_x^2 \\ k_y^2 \end{Bmatrix} - \begin{Bmatrix} \Phi_1 \\ \Phi_2 \\ 0 \\ \Phi_3 \\ \Phi_4 \\ 0 \\ \Phi_5 \\ \Phi_6 \\ 0 \\ 0 \\ 0 \\ 0 \\ 0 \end{Bmatrix} \tag{15}$$

$$\begin{aligned}
 \varepsilon_x^0 &= I_{11} \frac{\partial^2 f}{\partial y^2} - I_{12} \frac{\partial^2 f}{\partial x^2} + I_{13} \frac{\partial \phi_x}{\partial x} \\
 &\quad + I_{14} \frac{\partial \phi_y}{\partial y} - c_1 I_{15} \left(\frac{\partial^2 w}{\partial x^2} + \frac{\partial \phi_x}{\partial x} \right) \\
 &\quad - c_1 I_{16} \left(\frac{\partial^2 w}{\partial y^2} + \frac{\partial \phi_y}{\partial y} \right) + I_{17} \Phi_1 + I_{18} \Phi_2, \\
 \varepsilon_y^0 &= I_{21} \frac{\partial^2 f}{\partial x^2} - I_{12} \frac{\partial^2 f}{\partial y^2} + I_{23} \frac{\partial \phi_x}{\partial x} + I_{24} \frac{\partial \phi_y}{\partial y} \\
 &\quad - c_1 I_{25} \left(\frac{\partial^2 w}{\partial x^2} + \frac{\partial \phi_x}{\partial x} \right) \\
 &\quad - c_1 I_{26} \left(\frac{\partial^2 w}{\partial y^2} + \frac{\partial \phi_y}{\partial y} \right) + I_{27} \Phi_1 + I_{28} \Phi_2, \\
 \gamma_{xy}^0 &= -I_{31} \frac{\partial^2 f}{\partial x \partial y} + I_{32} \left(\frac{\partial \phi_x}{\partial y} + \frac{\partial \phi_y}{\partial x} \right) \\
 &\quad - c_1 I_{33} \left(2 \frac{\partial^2 w}{\partial x \partial y} + \frac{\partial \phi_x}{\partial y} + \frac{\partial \phi_y}{\partial x} \right),
 \end{aligned} \tag{17}$$

with the detail of coefficients $I_{ij}(i = \overline{1, 2}, j = \overline{1, 8})$, $I_{3k}(k = \overline{1, 3})$ are given in “Appendix A”.

The Airy’s stress function $f(x, y, t)$ is introduced as

$$N_x = \frac{\partial^2 f}{\partial y^2}, N_y = \frac{\partial^2 f}{\partial x^2}, N_{xy} = -\frac{\partial^2 f}{\partial x \partial y}. \tag{18}$$

7 The nonlinear motion equations and the geometrical compatibility equation

7.1 The nonlinear motion equations

The nonlinear motion equations the carbon nanotube polymer composite elliptical cylindrical shells are (Brush and Almroth 1975; Reddy 2004)

$$\frac{\partial N_x}{\partial x} + \frac{\partial N_{xy}}{\partial y} = \bar{I}_1 \frac{\partial^2 u}{\partial t^2} + \bar{I}_2 \frac{\partial^2 \phi_x}{\partial t^2} - \bar{I}_3 \frac{\partial^3 w}{\partial t^2 \partial x}, \tag{19a}$$

$$\frac{\partial N_{xy}}{\partial x} + \frac{\partial N_y}{\partial y} = \bar{I}_1^* \frac{\partial^2 v}{\partial t^2} + \bar{I}_2^* \frac{\partial^2 \phi_y}{\partial t^2} - \bar{I}_3^* \frac{\partial^3 w}{\partial t^2 \partial y}, \tag{19b}$$

$$\begin{aligned}
 &\frac{\partial Q_x}{\partial x} + \frac{\partial Q_y}{\partial y} - 3c_1 \left(\frac{\partial R_x}{\partial x} + \frac{\partial R_y}{\partial y} \right) \\
 &\quad + c_1 \left(\frac{\partial^2 P_x}{\partial x^2} + 2 \frac{\partial^2 P_{xy}}{\partial x \partial y} + \frac{\partial^2 P_y}{\partial y^2} \right) + \frac{N_y}{R} + q + N_x \frac{\partial^2 w}{\partial x^2} \\
 &\quad + 2N_{xy} \frac{\partial^2 w}{\partial x \partial y} + N_y \frac{\partial^2 w}{\partial y^2} - k_1 w + k_2 \nabla^2 w = I_1 \frac{\partial^2 w}{\partial t^2} \\
 &\quad + 2\varepsilon I_1 \frac{\partial w}{\partial t} + \bar{I}_3 \frac{\partial^3 u}{\partial t^2 \partial x} + \bar{I}_5 \frac{\partial^3 \phi_x}{\partial t^2 \partial x} \\
 &\quad + \bar{I}_3^* \frac{\partial^3 v}{\partial t^2 \partial y} + \bar{I}_5^* \frac{\partial^3 \phi_y}{\partial t^2 \partial y} - c_1^2 I_7 \left(\frac{\partial^4 w}{\partial t^2 \partial x^2} + \frac{\partial^4 w}{\partial t^2 \partial y^2} \right),
 \end{aligned} \tag{19c}$$

$$\begin{aligned}
 &\frac{\partial M_x}{\partial x} + \frac{\partial M_{xy}}{\partial y} - Q_x + 3c_1 R_x - c_1 \left(\frac{\partial P_x}{\partial x} + \frac{\partial P_{xy}}{\partial y} \right) \\
 &\quad = \bar{I}_2 \frac{\partial^2 u}{\partial t^2} + \bar{I}_4 \frac{\partial^2 \phi_x}{\partial t^2} - \bar{I}_5 \frac{\partial^3 w}{\partial t^2 \partial x},
 \end{aligned} \tag{19d}$$

$$\begin{aligned}
 &\frac{\partial M_{xy}}{\partial x} + \frac{\partial M_y}{\partial y} - Q_y + 3c_1 R_y - c_1 \left(\frac{\partial P_{xy}}{\partial x} + \frac{\partial P_y}{\partial y} \right) \\
 &\quad = \bar{I}_2^* \frac{\partial^2 v}{\partial t^2} + \bar{I}_4^* \frac{\partial^2 \phi_y}{\partial t^2} - \bar{I}_5^* \frac{\partial^3 w}{\partial t^2 \partial y},
 \end{aligned} \tag{19e}$$

with q is an uniformly distributed pressure, ε is the viscous damping coefficient and the detail of coefficients $\bar{I}_i(i = \overline{1, 5})$, $\bar{I}_j^*(j = \overline{1, 5})$ may be found in “Appendix B”.

Substituting Eq. (18) into Eqs. (19a) and (19b) gives

$$\frac{\partial^2 u}{\partial t^2} = -\frac{\bar{I}_2}{\bar{I}_1} \frac{\partial^2 \phi_x}{\partial t^2} + \frac{\bar{I}_3}{\bar{I}_1} \frac{\partial^3 w}{\partial t^2 \partial x}, \tag{20a}$$

$$\frac{\partial^2 v}{\partial t^2} = -\frac{\bar{I}_2^*}{\bar{I}_1^*} \frac{\partial^2 \phi_y}{\partial t^2} + \frac{\bar{I}_3^*}{\bar{I}_1^*} \frac{\partial^3 w}{\partial t^2 \partial y}. \tag{20b}$$

Replacing Eqs. (20a), (20b) into Eqs. (19c)–(19e) leads to

$$\begin{aligned}
& \frac{\partial Q_x}{\partial x} + \frac{\partial Q_y}{\partial y} - 3c_1 \left(\frac{\partial R_x}{\partial x} + \frac{\partial R_y}{\partial y} \right) \\
& + c_1 \left(\frac{\partial^2 P_x}{\partial x^2} + 2 \frac{\partial^2 P_{xy}}{\partial x \partial y} + \frac{\partial^2 P_y}{\partial y^2} \right) + \frac{1}{R} \frac{\partial^2 f}{\partial x^2} \\
& + p + \frac{\partial^2 f}{\partial y^2} \frac{\partial^2 w}{\partial x^2} - 2 \frac{\partial^2 f}{\partial x \partial y} \frac{\partial^2 w}{\partial x \partial y} + \frac{\partial^2 f}{\partial x^2} \frac{\partial^2 w}{\partial y^2} \\
& - k_1 w + k_2 \nabla^2 w = I_1 \frac{\partial^2 w}{\partial t^2} + 2\varepsilon I_1 \frac{\partial w}{\partial t} + \bar{I}_5 \frac{\partial^3 \phi_x}{\partial t^2 \partial x} \\
& + \bar{I}_5^* \frac{\partial^3 \phi_y}{\partial t^2 \partial y} + \bar{I}_7 \frac{\partial^4 w}{\partial t^2 \partial x^2} + \bar{I}_7^* \frac{\partial^4 w}{\partial t^2 \partial y^2}, \\
& \frac{\partial M_x}{\partial x} + \frac{\partial M_{xy}}{\partial y} - Q_x + 3c_1 R_x - c_1 \left(\frac{\partial P_x}{\partial x} + \frac{\partial P_{xy}}{\partial y} \right) \\
& = \bar{I}_3 \frac{\partial^2 \phi_x}{\partial t^2} - \bar{I}_5 \frac{\partial^3 w}{\partial t^2 \partial x}, \\
& \frac{\partial M_{xy}}{\partial x} + \frac{\partial M_y}{\partial y} - Q_y + 3c_1 R_y - c_1 \left(\frac{\partial P_{xy}}{\partial x} + \frac{\partial P_y}{\partial y} \right) \\
& = \bar{I}_3^* \frac{\partial^2 \phi_y}{\partial t^2} - \bar{I}_5^* \frac{\partial^3 w}{\partial t^2 \partial y},
\end{aligned} \tag{21}$$

with

$$\begin{aligned}
\bar{I}_3 &= \left(\bar{I}_4 - \bar{I}_2 \frac{\bar{I}_2}{\bar{I}_1} \right), \bar{I}_3^* = \left(\bar{I}_4^* - \bar{I}_2^* \frac{\bar{I}_2^*}{\bar{I}_1^*} \right), \\
\bar{I}_5 &= \left(\bar{I}_5 - \bar{I}_2 \frac{\bar{I}_3}{\bar{I}_1} \right), \bar{I}_5^* = \left(\bar{I}_5^* - \bar{I}_2^* \frac{\bar{I}_3^*}{\bar{I}_1^*} \right) \\
\bar{I}_7 &= \left(\bar{I}_3 \frac{\bar{I}_3}{\bar{I}_1} - c_1^2 I_7 \right), \bar{I}_7^* = \left(\bar{I}_3^* \frac{\bar{I}_3^*}{\bar{I}_1^*} - c_1^2 I_7 \right)
\end{aligned} \tag{22}$$

7.2 The geometrical compatibility equation

The geometrical compatibility equation for an imperfect carbon nanotube polymer composite elliptical cylindrical shell is written as (Duc et al. 2015, 2016)

$$\begin{aligned}
& \frac{\partial^2 \varepsilon_x^0}{\partial y^2} + \frac{\partial^2 \varepsilon_y^0}{\partial x^2} - \frac{\partial^2 \gamma_{xy}^0}{\partial x \partial y} = \left(\frac{\partial^2 w}{\partial x \partial y} \right)^2 - \frac{\partial^2 w}{\partial x^2} \frac{\partial^2 w}{\partial y^2} \\
& + 2 \frac{\partial^2 w}{\partial x \partial y} \frac{\partial^2 w^*}{\partial x \partial y} - \frac{\partial^2 w}{\partial x^2} \frac{\partial^2 w^*}{\partial y^2} - \frac{\partial^2 w}{\partial y^2} \frac{\partial^2 w^*}{\partial x^2} - \frac{1}{R} \frac{\partial^2 w}{\partial x^2},
\end{aligned} \tag{23}$$

with function $w^*(x, y)$ denotes initial small imperfection of the shell.

Substitution of Eqs. (11) into Eqs. (15) and introducing the results into Eqs. (21) yields

$$\begin{aligned}
& L_{11}(w) + L_{12}(\phi_x) + L_{13}(\phi_y) + L_{14}(f) \\
& + S(w, f) + q = I_1 \frac{\partial^2 w}{\partial t^2} + 2\varepsilon I_1 \frac{\partial w}{\partial t} \\
& + \bar{I}_5 \frac{\partial^3 \phi_x}{\partial t^2 \partial x} + \bar{I}_5^* \frac{\partial^3 \phi_y}{\partial t^2 \partial y} + \bar{I}_7 \frac{\partial^4 w}{\partial t^2 \partial x^2} + \bar{I}_7^* \frac{\partial^4 w}{\partial t^2 \partial y^2}, \\
& L_{21}(w) + L_{22}(\phi_x) + L_{23}(\phi_y) + L_{24}(f) = \bar{I}_3 \frac{\partial^2 \phi_x}{\partial t^2} \\
& - \bar{I}_5 \frac{\partial^3 w}{\partial t^2 \partial x}, \\
& L_{31}(w) + L_{32}(\phi_x) + L_{33}(\phi_y) + L_{34}(f) \\
& = \bar{I}_3^* \frac{\partial^2 \phi_y}{\partial t^2} - \bar{I}_5^* \frac{\partial^3 w}{\partial t^2 \partial y},
\end{aligned} \tag{24}$$

in which

$$\begin{aligned}
L_{11}(w) &= X_{11} \frac{\partial^2 w}{\partial x^2} + X_{12} \frac{\partial^2 w}{\partial y^2} + X_{13} \frac{\partial^4 w}{\partial x^4} \\
& + X_{14} \frac{\partial^4 w}{\partial x^2 \partial y^2} + X_{15} \frac{\partial^4 w}{\partial y^4} - k_1 w \\
& + k_2 \left(\frac{\partial^2 w}{\partial x^2} + \frac{\partial^2 w}{\partial y^2} \right), \\
L_{12}(\phi_x) &= X_{11} \frac{\partial \phi_x}{\partial x} + X_{16} \frac{\partial^3 \phi_x}{\partial x^3} + X_{17} \frac{\partial^3 \phi_x}{\partial x \partial y^2}, \\
L_{13}(\phi_y) &= X_{12} \frac{\partial \phi_y}{\partial y} + X_{18} \frac{\partial^3 \phi_y}{\partial y^3} + X_{19} \frac{\partial^3 \phi_y}{\partial x^2 \partial y}, \\
L_{14}(f) &= X_{110} \frac{\partial^4 f}{\partial x^4} + X_{111} \frac{\partial^4 f}{\partial x^2 \partial y^2} + X_{112} \frac{\partial^4 f}{\partial y^4},
\end{aligned}$$

$$\begin{aligned}
 S(w, f) &= \frac{\partial^2 f}{\partial y^2} \frac{\partial^2 w}{\partial x^2} - 2 \frac{\partial^2 f}{\partial x \partial y} \frac{\partial^2 w}{\partial y^2} + \frac{\partial^2 f}{\partial x^2} \frac{\partial^2 w}{\partial y^2} + \frac{1}{R} \frac{\partial^2 f}{\partial x^2}, \\
 L_{21}(w) &= X_{21} \frac{\partial w}{\partial x} + X_{22} \frac{\partial^3 w}{\partial x^3} + X_{23} \frac{\partial^3 w}{\partial x \partial y^2}, \\
 L_{22}(\phi_x) &= X_{21} \phi_x + X_{24} \frac{\partial^2 \phi_x}{\partial x^2} + X_{25} \frac{\partial^2 \phi_x}{\partial y^2}, \\
 L_{23}(\phi_y) &= X_{26} \frac{\partial^2 \phi_y}{\partial x \partial y}, \\
 L_{24}(f) &= X_{27} \frac{\partial^3 f}{\partial x^3} + X_{28} \frac{\partial^3 f}{\partial x \partial y^2}, \\
 L_{31}(w) &= X_{31} \frac{\partial w}{\partial y} + X_{32} \frac{\partial^3 w}{\partial x^2 \partial y} + X_{33} \frac{\partial^3 w}{\partial y^3}, \\
 L_{32}(\phi_x) &= X_{34} \frac{\partial^2 \phi_x}{\partial x \partial y}, \\
 L_{33}(\phi_y) &= X_{31} \phi_y + X_{35} \frac{\partial^2 \phi_y}{\partial x^2} + X_{36} \frac{\partial^2 \phi_y}{\partial y^2}, \\
 L_{34}(f) &= X_{37} \frac{\partial^3 f}{\partial x^2 \partial y} + X_{38} \frac{\partial^3 f}{\partial y^3},
 \end{aligned}
 \tag{25}$$

and the detail of coefficients $X_{1i}(i = \overline{1, 12})$, $X_{2j}(j = \overline{1, 8})$, $X_{3k}(k = \overline{1, 8})$ may be found in “Appendix C”.

For an imperfect the carbon nanotube polymer composite elliptical cylindrical shell, Eqs. (24) may be transformed to the form as

$$\begin{aligned}
 &L_{11}(w) + L_{12}(\phi_x) + L_{13}(\phi_y) + L_{14}(f) + S(w, f) \\
 &+ S^*(w^*, f) + q = I_1 \frac{\partial^2 w}{\partial t^2} + 2\epsilon I_1 \frac{\partial w}{\partial t} \\
 &+ \overline{I}_5 \frac{\partial^3 \phi_x}{\partial t^2 \partial x} + \overline{I}_5^* \frac{\partial^3 \phi_y}{\partial t^2 \partial y} + \overline{I}_7 \frac{\partial^4 w}{\partial t^2 \partial x^2} + \overline{I}_7^* \frac{\partial^4 w}{\partial t^2 \partial y^2}, \\
 &L_{21}(w) + L_{22}(\phi_x) + L_{23}(\phi_y) + L_{24}(f) \\
 &+ L_{21}^*(w^*) = \overline{I}_3 \frac{\partial^2 \phi_x}{\partial t^2} - \overline{I}_5 \frac{\partial^3 w}{\partial t^2 \partial x}, \\
 &L_{31}(w) + L_{32}(\phi_x) + L_{33}(\phi_y) + L_{34}(f) \\
 &+ L_{31}^*(w^*) = \overline{I}_3^* \frac{\partial^2 \phi_y}{\partial t^2} - \overline{I}_5^* \frac{\partial^3 w}{\partial t^2 \partial y},
 \end{aligned}
 \tag{26}$$

in which

$$\begin{aligned}
 L_{11}^*(w^*) &= X_{11} \frac{\partial^2 w^*}{\partial x^2} + X_{12} \frac{\partial^2 w^*}{\partial y^2}, \quad S^*(w^*, f) \\
 &= \frac{\partial^2 f}{\partial y^2} \frac{\partial^2 w^*}{\partial x^2} - 2 \frac{\partial^2 f}{\partial x \partial y} \frac{\partial^2 w^*}{\partial x \partial y} + \frac{\partial^2 f}{\partial x^2} \frac{\partial^2 w^*}{\partial y^2}, \\
 L_{21}^*(w^*) &= X_{21} \frac{\partial w^*}{\partial x}, \quad L_{31}^*(w^*) = X_{31} \frac{\partial w^*}{\partial y},
 \end{aligned}
 \tag{27}$$

Introduction of Eqs. (17) into Eq. (23) gives the compatibility equation of the imperfect the carbon nanotube polymer composite elliptical cylindrical shell as

$$\begin{aligned}
 &I_{21} \frac{\partial^4 f}{\partial x^4} + I_{11} \frac{\partial^4 f}{\partial y^4} + J_1 \frac{\partial^4 f}{\partial x^2 \partial y^2} + J_2 \frac{\partial^3 \phi_x}{\partial x^3} + J_3 \frac{\partial^3 \phi_x}{\partial x \partial y^2} + J_4 \frac{\partial^3 \phi_y}{\partial y^3} \\
 &+ J_5 \frac{\partial^3 \phi_y}{\partial y \partial x^2} - c_{1I_{25}} \frac{\partial^4 w}{\partial x^4} - c_{1I_{16}} \frac{\partial^4 w}{\partial y^4} + J_6 \frac{\partial^4 w}{\partial x^2 \partial y^2} \\
 &- \left(\frac{\partial^2 w^2}{\partial x \partial y} - \frac{\partial^2 w \partial^2 w}{\partial x^2 \partial y^2} + 2 \frac{\partial^2 w \partial^2 w^*}{\partial x \partial y \partial x \partial y} - \frac{\partial^2 w \partial^2 w^*}{\partial x^2 \partial y^2} - \frac{\partial^2 w \partial^2 w^*}{\partial y^2 \partial x^2} - \frac{1}{R} \frac{\partial^2 w}{\partial x^2} \right) \\
 &= 0
 \end{aligned}
 \tag{28}$$

where the detail of coefficients $J_i(i = \overline{1, 6})$ are represented in “Appendix D”.

Equations (26) and (28) are nonlinear governing equations in terms of four variables w , ϕ_x , ϕ_y and f and they are used to study the nonlinear dynamic response and vibration of the imperfect carbon nanotube polymer composite elliptical cylindrical shells. Specifically, the natural frequency and the deflection–time curves could be determined from this equations system.

8 Boundary conditions and approximate solutions

8.1 Boundary conditions

In the present study, the edges of the carbon nanotube polymer composite elliptical cylindrical shells are assumed to be simply supported and immovable. The boundary conditions in this case are

$$w = u = M_x = 0, \quad N_x = N_{x0} \text{ at } x = 0 \text{ and } x = L,
 \tag{29}$$

where N_{x0} is pre-buckling compressive force effect on edges $x = 0, L$.

8.2 Approximate solutions

Based on the boundary condition (29), the approximate solutions are assumed to be the forms as (Duc et al. 2015)

$$\begin{aligned} w(x, y, t) &= W(t) \sin \lambda_m x \sin \delta_n y, \\ \phi_x(x, y, t) &= \Phi_x(t) \cos \lambda_m x \sin \delta_n y, \\ \phi_y(x, y, t) &= \Phi_y(t) \sin \lambda_m x \cos \delta_n y, \end{aligned} \tag{30}$$

in which $\lambda_m = m\pi/L, \delta_n = n/R; m, n$ are odd natural numbers and W, Φ_x, Φ_y are amplitude of the deflection and rotation angle, respectively.

In this study, we assume that the initial imperfection w^* has the same form with the shell deflection, i.e.

$$w^*(x, y, t) = W_0 \sin \lambda_m x \sin \delta_n y, \tag{31}$$

where W_0 is amplitude of the imperfect function.

Composing Eqs. (30) and (31) into Eq. (28) then solving obtained equation for unknown variable f leads to

$$\begin{aligned} f(x, y, t) &= P_1(t) \cos 2\lambda_m x + P_2(t) \cos 2\delta_n y \\ &\quad + P_3(t) \sin \lambda_m x \sin \delta_n y + \frac{1}{2} N_{x0} y^2, \end{aligned} \tag{32}$$

with

$$\begin{aligned} P_1 &= \frac{\delta_n^2}{32I_{21}\lambda_m^2} W(W + 2\mu h), \\ P_2 &= \frac{\lambda_m^2}{32I_{11}\delta_n^2} W(W + 2\mu h), \\ P_3 &= Q_1 W + Q_2 \Phi_x + Q_3 \Phi_y, \end{aligned} \tag{33}$$

and

$$\begin{aligned} Q_1 &= \frac{\frac{\lambda_m^2}{R} + c_1 I_{25} \lambda_m^4 + c_1 I_{16} \delta_n^4 - J_6 \lambda_m^2 \delta_n^2}{I_{21} \lambda_m^4 + J_1 \lambda_m^2 \delta_n^2 + I_{11} \delta_n^4}, \\ Q_2 &= \frac{-(J_2 \lambda_m^3 + J_3 \lambda_m \delta_n^2)}{I_{21} \lambda_m^4 + J_1 \lambda_m^2 \delta_n^2 + I_{11} \delta_n^4}, \\ Q_3 &= \frac{-(J_4 \delta_n^3 + J_5 \lambda_m^2 \delta_n)}{I_{21} \lambda_m^4 + J_1 \lambda_m^2 \delta_n^2 + I_{11} \delta_n^4}. \end{aligned} \tag{34}$$

9 Vibration analysis

Substituting Eqs. (30)–(32) into Eqs. (26) and using the Galerkin method to the resulting equations gives

$$\begin{aligned} &r_{11} W + r_{12} \Phi_x + r_{13} \Phi_y + r_{14} (W + \mu h) \Phi_x \\ &\quad + r_{15} (W + \mu h) \Phi_y + [n_1 - N_{x0} \lambda_m^2] (W + \mu h) \\ &\quad + n_2 W (W + \mu h) + n_3 W (W + 2\mu h) \\ &\quad + n_4 W (W + \mu h) (W + 2\mu h) \\ &\quad + n_5 q = I_0 \frac{\partial^2 W}{\partial t^2} + 2EI_1 \frac{\partial W}{\partial t} - \lambda_m \bar{I}_5 \frac{\partial^2 \Phi_x}{\partial t^2} \\ &\quad - \delta_n \bar{I}_5^* \frac{\partial^2 \Phi_y}{\partial t^2}, \\ &r_{21} W + r_{22} \Phi_x + r_{23} \Phi_y + n_6 (W + \mu h) \\ &\quad + n_7 W (W + 2\mu h) = \bar{I}_3 \frac{\partial^2 \Phi_x}{\partial t^2} - \lambda_m \bar{I}_5 \frac{\partial^2 W}{\partial t^2}, \\ &r_{31} W + r_{32} \Phi_x + r_{33} \Phi_y + n_8 (W + \mu h) \\ &\quad + n_9 W (W + 2\mu h) = \bar{I}_3^* \frac{\partial^2 \Phi_y}{\partial t^2} - \delta_n \bar{I}_5^* \frac{\partial^2 W}{\partial t^2}, \end{aligned} \tag{35}$$

in which the coefficients $r_{1i} (i = \overline{1, 3}), r_{jk} (j = \overline{2, 3}, k = \overline{1, 2}), n_m (m = \overline{1, 9})$ are given in ‘‘Appendix E’’.

9.1 Temperature field

The condition showing the immovability of the edges of the carbon nanotube polymer composite elliptical cylindrical shells is satisfied in an average sense as (Duc et al. 2015)

$$\int_0^{2\pi R} \int_0^L \frac{\partial u}{\partial x} dx dy = 0. \tag{36}$$

Form Eqs. (11) and (17) we have

$$\begin{aligned} \frac{\partial u}{\partial x} &= I_{11} f_{,yy} - I_{12} f_{,xx} - I_{13} \phi_{,x,x} + I_{14} \phi_{,y,y} \\ &\quad + c_1 I_{15} (\phi_{,x,x} + w_{,xx}) \\ &\quad - c_1 I_{16} (\phi_{,y,y} + w_{,yy}) + I_{17} \Phi_1 \\ &\quad + I_{18} \Phi_2 - \frac{1}{2} \left(\frac{\partial w}{\partial x} \right)^2 - \frac{\partial w}{\partial x} \frac{\partial w^*}{\partial x}. \end{aligned} \tag{37}$$

Replacing Eqs. (30)–(32) into Eq. (37) and substituting the results into Eq. (36) gives

$$N_{x0} = \frac{\lambda_m^2}{8I_{11}} W(W + 2W_0) - \frac{I_{17}}{I_{11}} \Phi_1 - \frac{I_{18}}{I_{11}} \Phi_2. \tag{38}$$

9.2 Nonlinear deflection amplitude–time curves

Assume that the carbon nanotube polymer composite elliptical cylindrical shells subjected to uniformly

distributed transverse load $q = Q \sin \Omega t$ (Q is the amplitude of uniformly excited load, Ω is the frequency of the load). Introduction of Eqs. (38) into Eq. (35) gives

$$\begin{aligned}
 & r_{11}W + r_{12}\Phi_x + r_{13}\Phi_y + r_{14}(W + W_0)\Phi_x \\
 & + r_{15}(W + W_0)\Phi_y \\
 & + n_1^*(W + W_0) + n_2W(W + W_0) \\
 & + n_3W(W + 2W_0) + n_4^*W(W + W_0)(W + 2W_0) \\
 & + n_5Q \sin \Omega t \\
 & = I_0 \frac{\partial^2 W}{\partial t^2} + 2\varepsilon I_1 \frac{\partial W}{\partial t} - \lambda_m \bar{I}_5 \frac{\partial^2 \Phi_x}{\partial t^2} - \delta_n \bar{I}_5^* \frac{\partial^2 \Phi_y}{\partial t^2}, \\
 & r_{21}W + r_{22}\Phi_x + r_{23}\Phi_y + n_6(W + W_0) \\
 & + n_7W(W + 2W_0) = \bar{I}_3 \frac{\partial^2 \Phi_x}{\partial t^2} - \lambda_m \bar{I}_5 \frac{\partial^2 W}{\partial t^2}, \\
 & r_{31}W + r_{32}\Phi_x + r_{33}\Phi_y + n_8(W + W_0) \\
 & + n_9W(W + 2W_0) = \bar{I}_3^* \frac{\partial^2 \Phi_y}{\partial t^2} - \delta_n \bar{I}_5^* \frac{\partial^2 W}{\partial t^2},
 \end{aligned} \tag{39}$$

where

$$n_1^* = n_1 + \lambda_m^2 \left(\frac{I_{17}}{I_{11}} \Phi_1 + \frac{I_{18}}{I_{11}} \Phi_2 \right), n_4^* = n_4 - \frac{\lambda_m^4}{8I_{11}}. \tag{40}$$

Equation (39) is the nonlinear governing equation which is used to study the nonlinear vibration for the imperfect carbon nanotube polymer composite elliptical cylindrical shells with immovable edges. The fourth-order Runge–Kutta method is applied to solve Eq. (39). The initial conditions are given as

$$\begin{aligned}
 & W(0) = 0, \frac{dW}{dt}(0) = 0, \Phi_x(0) = 0, \\
 & \frac{d\Phi_x}{dt}(0) = 0, \Phi_y(0) = 0, \frac{d\Phi_y}{dt}(0) = 0.
 \end{aligned} \tag{41}$$

Table 3 Comparison of dimensionless frequencies $\varpi = \Omega(h/\pi)\sqrt{2(1+\nu)\rho/E}$ for an isotropic cylindrical shell

(m, n)	(1,1)	(1,2)	(1,3)	(1,4)
Lam and Loy (1995)	0.03748	0.03671	0.03635	0.03720
Xuebin (2008)	0.03739	0.03666	0.03634	0.03723
Shen (2012)	0.03712	0.03648	0.03620	0.03700
Present	0.03717	0.03654	0.03627	0.03709

9.3 Natural frequencies

In the absence of external forces and viscous damping, the natural frequencies of the perfect shell can be determined by solving the following equation

$$\begin{vmatrix}
 l_{11} + n_1^* + I_0\omega^2 & l_{12} - \lambda_m \bar{I}_5 \omega^2 & l_{13} - \delta_n \bar{I}_5^* \omega^2 \\
 l_{21} + n_6 - \lambda_m \bar{I}_5 \omega^2 & l_{22} + \bar{I}_3 \omega^2 & l_{23} \\
 l_{31} + n_8 - \delta_n \bar{I}_5^* \omega^2 & l_{32} & l_{33} + \bar{I}_3^* \omega^2
 \end{vmatrix} = 0. \tag{42}$$

Three values of natural frequencies are obtained from Eq. (42) and the lowest value of them is considered.

10 Numerical results and discussion

10.1 Comparison studies

To verify the accuracy of the present method, the dimensionless frequencies of isotropic cylindrical shell are calculated and compared in Table 3 with the results presented by Lam and Loy (1995) based on Love’s first approximation theory, Xuebin (2008) using the Flugge classical thin shell theory and Shen (2012) based on the higher order shear deformation shell theory with the material properties and the geometrical parameters are chosen as $E = 210$ GPa, $\nu = 0.3$, $\rho = 7850$ kg/m³, $R/L = 2$, $h/R = 0.06$. The results from the Table 3 show that a good agreement is obtained in this comparison.

Next, Table 4 shows the comparison of fundamental frequencies of the carbon nanotube polymer composite elliptical cylindrical shells using the higher order shear deformation theory in this paper with the results of Shen and Xiang (2012) in cases of two values of ratio $\bar{Z} = L^2/Rh$. The geometric parameters of the shell are chosen as $R/h = 10$, $(m, n) = (1, 1)$, $h = 5$ mm. Again, the results from this approach are so close with the existing results.

10.2 Natural frequency

The effects of temperature increment ΔT , geometrical parameter L/R and modes (m, n) on the natural

Table 4 Comparison of fundamental frequencies $\bar{\Omega} = \Omega(R^2/h)\sqrt{\rho_0/E_0}$ for the carbon nanotube polymer composite elliptical cylindrical shells ($T = 300\text{ K}$, $R/h = 10$, $(m, n) = (1, 1)$, $h = 5\text{ mm}$)

V_{CNT}^*	Type of reinforcement of carbon nanotube	$\bar{Z} = 100$		$\bar{Z} = 500$	
		Present	Shen and Xiang (2012)	Present	Shen and Xiang (2012)
0.12	UD	5.1051	5.0998	2.3672	2.3671
	V	5.0795	5.0951	2.3950	2.3979
	X	5.2331	5.2333	2.3876	2.3886
0.17	UD	6.5515	6.5462	3.0467	3.0456
	V	6.5489	6.5686	3.0924	3.0960
	X	6.7269	6.7292	3.0838	3.0848
0.28	UD	6.9906	6.9803	3.2223	3.2221
	V	7.0626	7.0597	3.3193	3.3132
	X	7.3320	7.3295	3.3318	3.3242

Table 5 Effects of temperature increment, L/R ratio and mode (m, n) on natural frequencies (s^{-1}) of the carbon nanotube polymer composite elliptical cylindrical shells

ΔT	L/R	(m, n)						
			(1,1)	(1,2)	(1,3)	(1,4)	(1,5)	(1,6)
0	1		6306.05	6615.57	7265.29	8147.67	9181.61	10,317.23
	1.5		5182.54	5568.31	6355.99	7363.66	8500.66	9719.32
	2		4693.16	5151.24	6012.96	7077.05	8256.64	9507.87
200	1		6068.89	6432.63	7118.00	8023.22	9072.03	10,216.85
	1.5		5023.19	5466.99	6280.82	7302.11	8446.38	9668.09
	2		4579.33	5088.19	5967.98	7040.27	8223.33	9474.83

Table 6 Effects of carbon nanotube volume fraction, ratio b/h , type of carbon nanotube reinforcement and elastic foundations on natural frequencies (s^{-1}) of the carbon nanotube polymer composite elliptical cylindrical shells

b/h	k_1, k_2	$V_{CNT}^* = 0.12$			$V_{CNT}^* = 0.17$		
		UD	V	X	UD	V	X
10	(0,0)	3240.3	3188.8	3337.7	4153.2	4111.8	4283.1
15	(0,0)	2084.2	2070.7	2122.0	2681.7	2678.7	2736.6
20	(0,0)	1541.2	1537.6	1560.5	1986.4	1991.7	2017.3
10	(0.3,0.02)	7140.9	7117.5	7185.7	7570.8	7548.0	7642.9
15	(0.3,0.02)	5423.0	5417.7	5437.6	5656.3	5654.8	5682.5
20	(0.3,0.02)	4694.4	4693.2	4700.7	4837.5	4839.7	4850.3

frequency of the carbon nanotube polymer composite elliptical cylindrical shells are considered in Table 5. It is clear that the value of the natural frequency of the shell increases when the values temperature increment ΔT , ratio L/R and modes (m, n) increase. Moreover, the lowest natural frequency corresponds to the modes of vibration of shells $(m, n) = (1, 1)$. Note that, this

mode will be used as a representative mode to investigate the natural frequencies and nonlinear dynamic responses of the carbon nanotube polymer composite elliptical cylindrical shells.

Table 6 shows influences of volume fraction of carbon nanotube V_{CNT}^* , geometrical parameter b/h , type of carbon nanotube reinforcement and elastic

Fig. 3 Influences of carbon nanotube volume fraction on the nonlinear deflection amplitude–time curves of the carbon nanotube polymer composite elliptical cylindrical shells

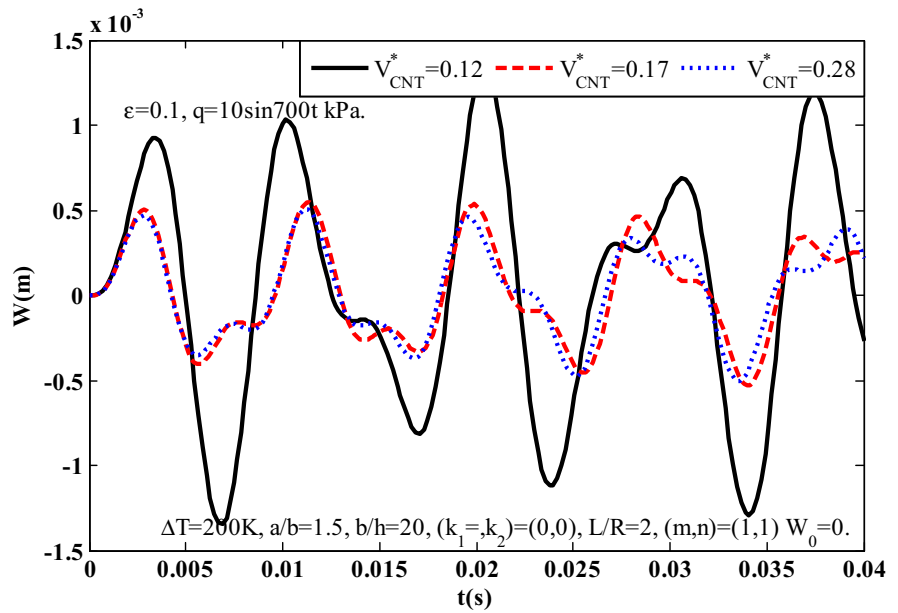
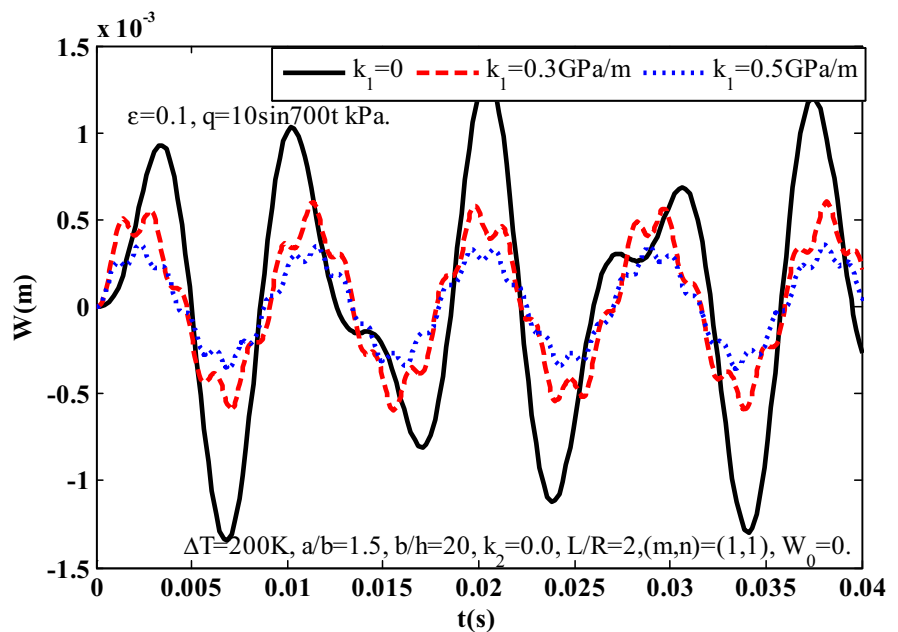


Fig. 4 Influences of the Winkler foundation on the nonlinear deflection amplitude–time curves of the carbon nanotube polymer composite elliptical cylindrical shells



foundations on the natural frequencies (s^{-1}) of the carbon nanotube polymer composite elliptical cylindrical shells. Clearly, the natural frequency of the nanocomposite elliptical cylindrical shell increases when the carbon nanotube volume fraction and the modulus k_1 (GPa/m), k_2 (GPa m) of elastic foundations increase and the ratio b/h decreases. Moreover, the carbon nanotube polymer composite elliptical

cylindrical shells with type carbon nanotube reinforcement X has the highest value of the natural frequency and the carbon nanotube polymer composite elliptical cylindrical shells with type carbon nanotube reinforcement V has the lowest value of the natural frequency of all.

Fig. 5 Influences of the Pasternak foundation on the nonlinear deflection amplitude–time curves of the carbon nanotube polymer composite elliptical cylindrical shells

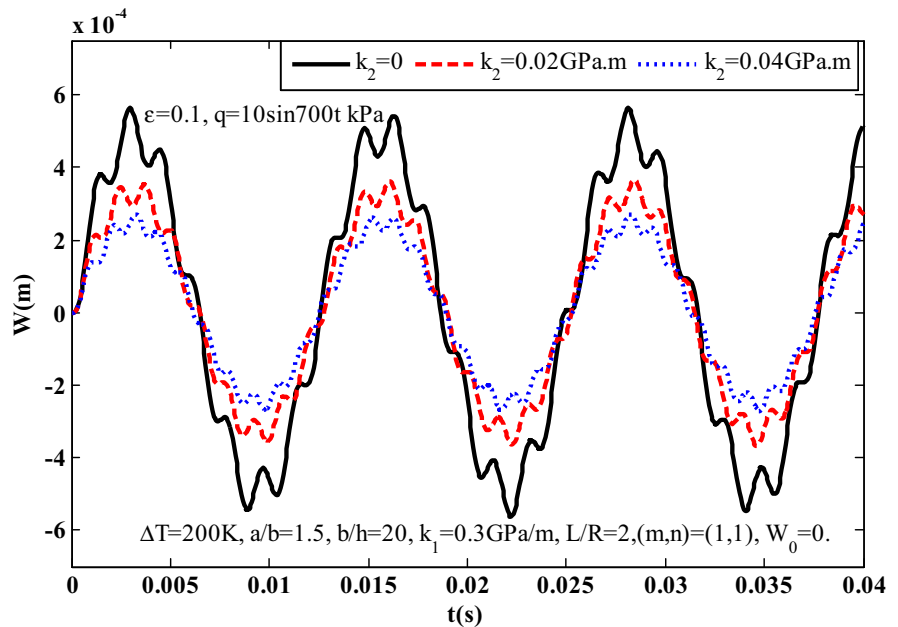
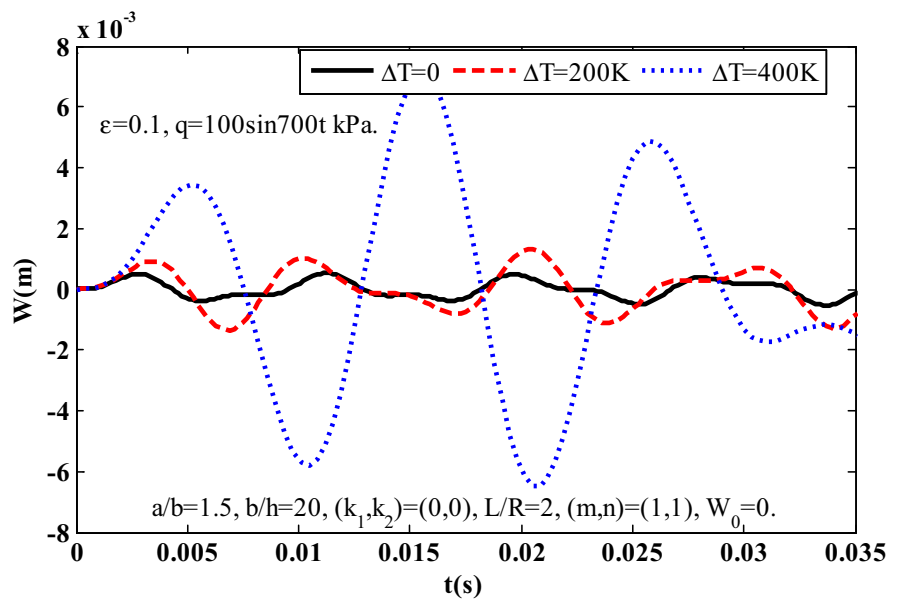


Fig. 6 Influences of temperature change ΔT on the nonlinear deflection amplitude–time curves of the carbon nanotube polymer composite elliptical cylindrical shells



10.3 Nonlinear deflection amplitude–time curves

Figure 3 describes the effect of carbon nanotube volume fraction V_{CNT}^* on the nonlinear deflection amplitude–time curves of the carbon nanotube polymer composite elliptical cylindrical shells with $b/h = 20$, $a/b = 1.5$, $L/R = 2$. We can see that the deflection amplitude of the carbon nanotube polymer composite elliptical cylindrical shells decreases when

the factor V_{CNT}^* increases. In other words, the carbon nanotube enhances the stiffness of the carbon nanotube polymer composite elliptical cylindrical shells.

Figures 4 and 5 show the effects of elastic foundations with two coefficients k_1 and k_2 on the nonlinear deflection amplitude–time curves of the carbon nanotube polymer composite elliptical cylindrical shells. From the figures, it is clear that the deflection amplitude of the nanocomposite elliptical cylindrical

Fig. 7 Influences of imperfection amplitude W_0 on the nonlinear deflection amplitude–time curves of the carbon nanotube polymer composite elliptical cylindrical shells

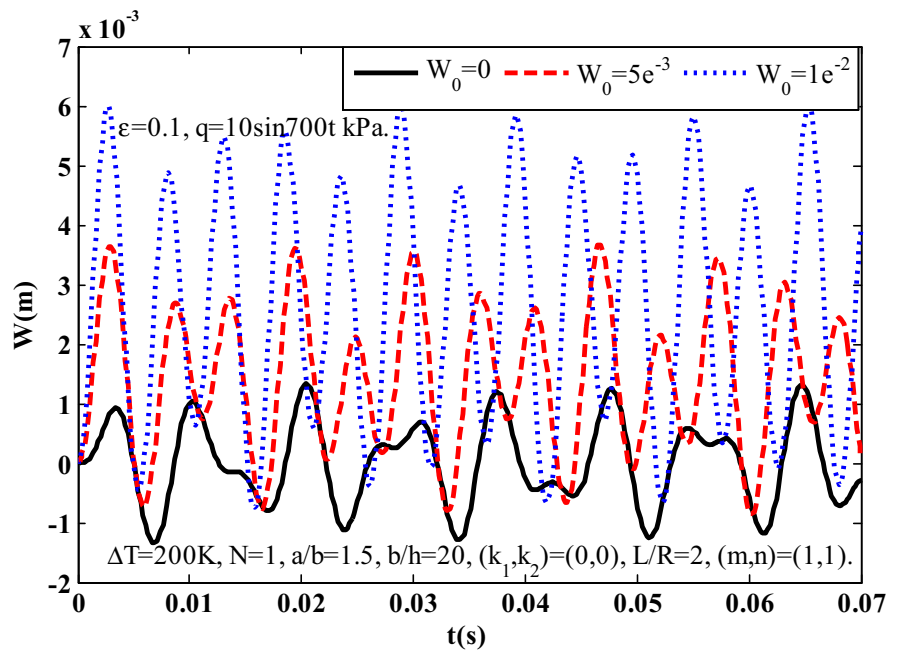
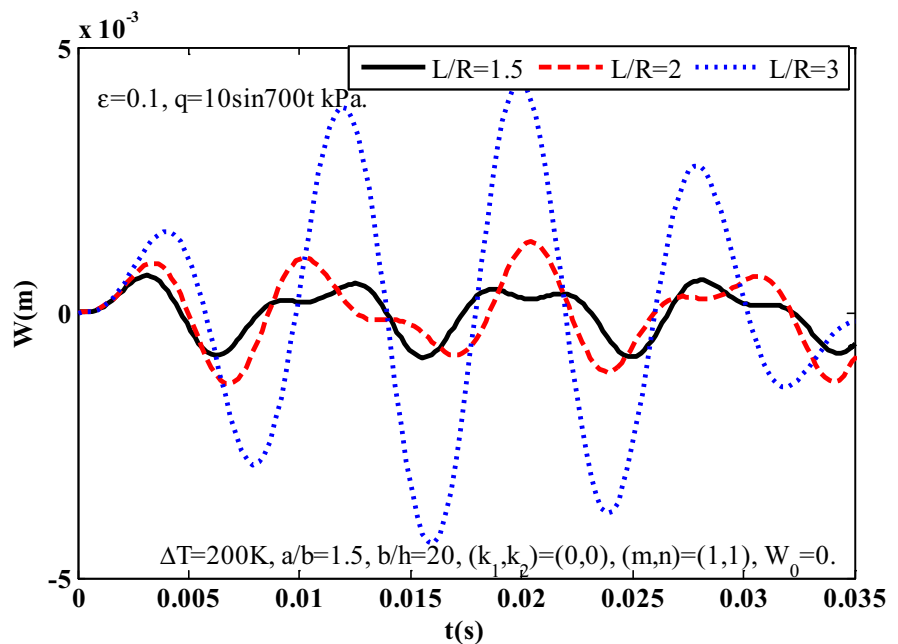


Fig. 8 Influences of factor L/R on the nonlinear deflection amplitude–time curves of the carbon nanotube polymer composite elliptical cylindrical shells



shell decreases significantly when the shell is rested on the elastic foundations. Furthermore, the beneficial effect of the Pasternak foundation with the shear layer stiffness k_2 on the nonlinear deflection amplitude–time curves of the carbon nanotube polymer composite elliptical cylindrical shells is stronger than the Winkler one with the modulus k_1 .

Figure 6 illustrates the effect of temperature change ΔT on the nonlinear deflection amplitude–time curves of the carbon nanotube polymer composite elliptical cylindrical shells. Three values of ΔT : 0, 200 K and 400 K are considered. Obviously, an increase of the temperature increment ΔT leads to an increase of the

Fig. 9 Influences of factor a/b on the nonlinear deflection amplitude–time curves of the carbon nanotube polymer composite elliptical cylindrical shells

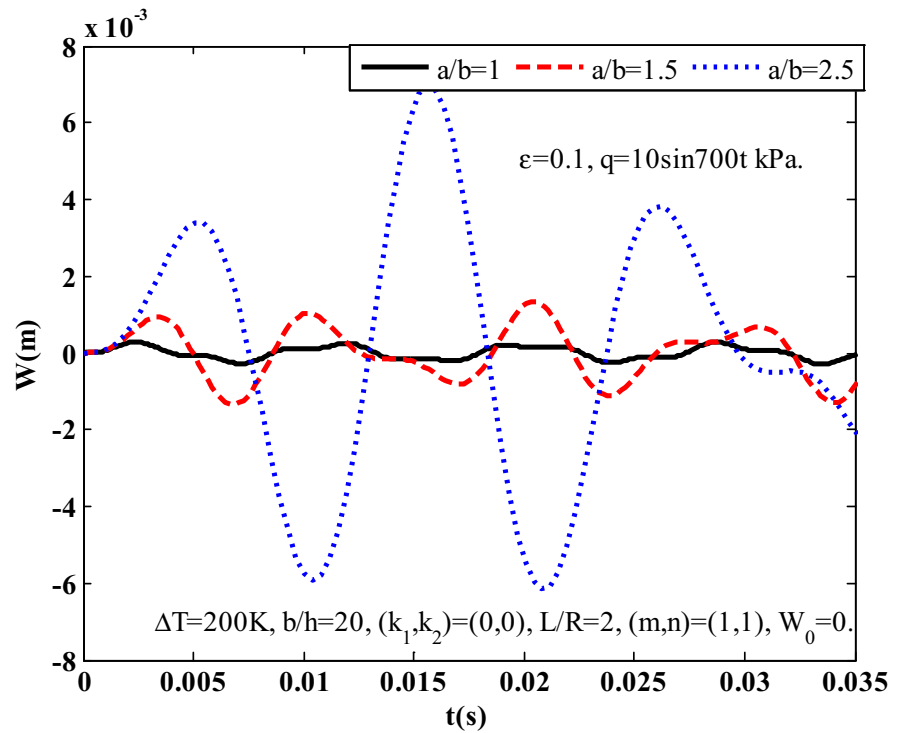
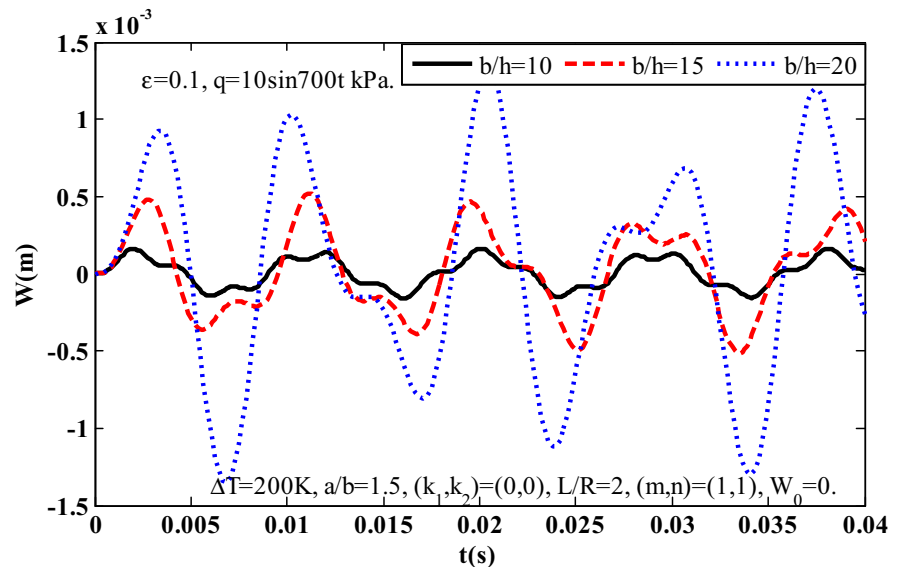


Fig. 10 Influences of factor b/h on the nonlinear deflection amplitude–time curves of the carbon nanotube polymer composite elliptical cylindrical shells

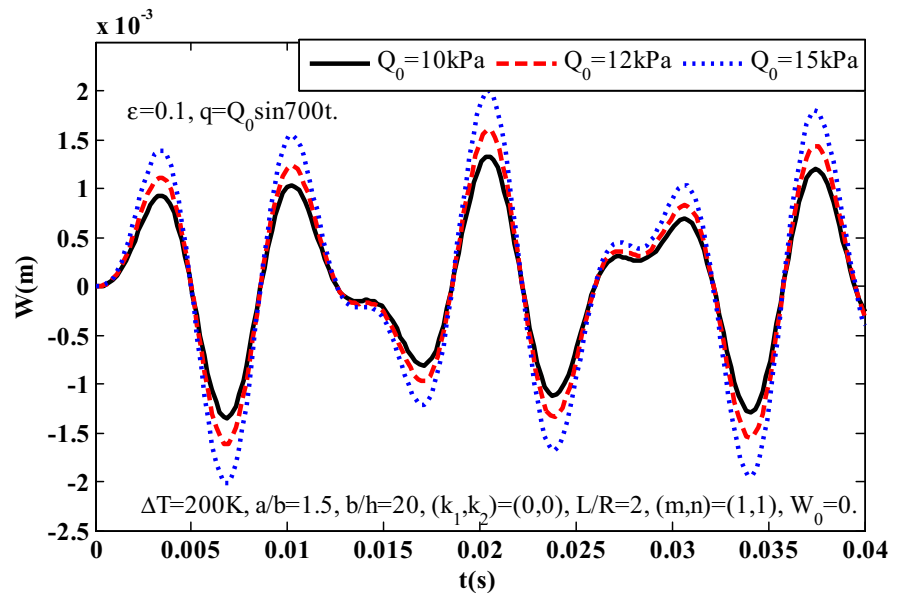


deflection amplitude of the carbon nanotube polymer composite elliptical cylindrical shells.

Figure 7 indicates the nonlinear deflection amplitude–time curves of the carbon nanotube polymer composite elliptical cylindrical shells with various values of the imperfection amplitude W_0 . As can be

observed, the imperfection amplitude has a strong effect on the nonlinear deflection amplitude–time curves of the carbon nanotube polymer composite elliptical cylindrical shells; the amplitude of the shell increases when the initial imperfection amplitude increases.

Fig. 11 Influences of excitation force amplitude Q_0 on the nonlinear deflection amplitude–time curves of the carbon nanotube polymer composite elliptical cylindrical shells



Figures 8, 9 and 10 give the influences of the geometrical factors L/R , a/b and b/h on the nonlinear deflection amplitude–time curves of the carbon nanotube polymer composite elliptical cylindrical shells, respectively. It can be seen that the fluctuation amplitude of the carbon nanotube polymer composite elliptical cylindrical shells increases when increasing the ratio L/R , a/b and b/h .

The effect of excitation force amplitude Q_0 on the nonlinear deflection amplitude–time curves of the carbon nanotube polymer composite elliptical cylindrical shells is shown in Fig. 11. As can be seen, the higher excitation force amplitude is, the higher vibration amplitude of the carbon nanotube polymer composite elliptical cylindrical shells is.

11 Concluding remarks

The nonlinear dynamic response and vibration of the carbon nanotube polymer composite elliptical cylindrical shells on elastic foundations subjected to the combination of the mechanical and thermal loads are presented in this paper. The material properties of the shells are supposed to depend on temperature and the shell thickness direction. The basic equations are derived based on the Reddy's higher order shear deformation shell theory. The Galerkin method and fourth-order Runge–Kutta method are used to

determine the natural frequencies and nonlinear deflection amplitude–time curves of the shells. The accuracy of present approach is also verified by comparing with the ones of other authors. From the obtained results in the study, there are some conclusions:

- The initial imperfection and temperature increment significant negative effect on the nonlinear vibration and dynamic response of the carbon nanotube polymer composite elliptical cylindrical shells. The deflection amplitude increases and the natural frequency decreases according to the increase of the initial imperfection amplitude and temperature increment.
- The elastic foundations dramatically enhance the natural frequencies and reduce the deflection amplitude of the carbon nanotube polymer composite elliptical cylindrical shells. Moreover, the influence of linear Winkler foundation is weaker than one of Pasternak foundation.
- The carbon nanotubes could be used to strengthen the mechanical properties of the carbon nanotube polymer composite elliptical cylindrical shells because they increase the natural frequencies and decrease the fluctuation amplitude of the shells.
- The geometrical parameters ratios have strongly effects on the nonlinear vibration and dynamic response of the carbon nanotube polymer composite elliptical cylindrical shells.

Funding This work has been supported/partly supported by Vietnam National University, Hanoi (VNU), under Project No. QG.18.37.

Compliance with Ethical Standards

Conflict of interest The authors declare no conflict of interest.

Appendix A

$$\begin{aligned}\Delta &= A_{11}A_{22} - A_{12}^2, I_{11} = \frac{A_{22}}{\Delta}, I_{12} = \frac{A_{12}}{\Delta}, \\ I_{13} &= \frac{B_{12}A_{12} - B_{11}A_{22}}{\Delta}, I_{14} = \frac{B_{22}A_{12} - B_{12}A_{22}}{\Delta}, \\ I_{15} &= \frac{E_{12}A_{12} - E_{11}A_{22}}{\Delta}, I_{16} = \frac{E_{22}A_{12} - E_{12}A_{22}}{\Delta}, \\ I_{17} &= \frac{A_{22}}{\Delta}, I_{18} = -\frac{A_{12}}{\Delta}, \\ I_{21} &= \frac{A_{11}}{\Delta}, I_{23} = \frac{B_{11}A_{12} - B_{12}A_{11}}{\Delta}, \\ I_{24} &= \frac{B_{12}A_{12} - B_{22}A_{11}}{\Delta}, I_{25} = \frac{E_{11}A_{12} - E_{12}A_{11}}{\Delta}, \\ I_{26} &= \frac{E_{12}A_{12} - E_{22}A_{11}}{\Delta}, I_{27} = -\frac{A_{12}}{\Delta}, I_{28} = \frac{A_{11}}{\Delta}, \\ I_{31} &= \frac{1}{A_{66}}, I_{32} = -\frac{B_{66}}{A_{66}}, I_{33} = -\frac{E_{66}}{A_{66}}.\end{aligned}$$

Appendix B

$$\begin{aligned}\bar{I}_1 &= I_1, \bar{I}_1^* = I_1 + \frac{2I_2}{R}, \bar{I}_2 = I_2 - c_1I_4, \\ \bar{I}_2^* &= I_2 + \frac{I_3}{R} - c_1I_4 - \frac{c_1I_5}{R}, \\ \bar{I}_3 &= c_1I_4, \bar{I}_3^* = c_1I_4 + \frac{c_1I_5}{R}, \bar{I}_4 = \bar{I}_4^* = I_3 - 2c_1I_5 \\ &+ c_1^2I_7, \bar{I}_5 = \bar{I}_5^* = c_1I_5 - c_1^2I_7.\end{aligned}$$

Appendix C

$$\begin{aligned}X_{11} &= A_{44} - 6c_1D_{44} + 9c_1^2F_{44}, X_{12} = A_{55} - 6c_1D_{55} + 9c_1^2F_{55}, \\ X_{13} &= -c_1^2(E_{11}I_{15} + E_{12}I_{25} + H_{11}), \\ X_{14} &= -c_1^2(4E_{66}I_{33} + 4H_{66} + E_{11}I_{16} + E_{12}I_{26} \\ &+ 2H_{12} + E_{12}I_{15} + E_{22}I_{25}), \\ X_{15} &= -c_1^2(E_{12}I_{16} + E_{22}I_{26} + H_{22}), \\ X_{16} &= c_1(E_{11}I_{13} - c_1E_{11}I_{15} + F_{11} \\ &- c_1H_{11} + E_{12}I_{23} - c_1E_{12}I_{25}), \\ X_{17} &= c_1(2E_{66}I_{32} - 2c_1E_{66}I_{33} + 2F_{66} - 2c_1H_{66} \\ &+ c_1E_{12}I_{13} - c_1E_{12}I_{15} + F_{12} - c_1H_{12} \\ &+ E_{22}I_{23} - c_1E_{22}I_{25}), \\ X_{18} &= c_1(E_{12}I_{14} - c_1E_{12}I_{16} + E_{22}I_{24} - c_1E_{22}I_{26} + F_{22} - c_1H_{22}), \\ X_{19} &= c_1(2E_{66}I_{32} - 2c_1E_{66}I_{33} + 2F_{66} - 2c_1H_{66} + E_{11}I_{14} \\ &- c_1E_{11}I_{16} + E_{12}I_{24} - c_1E_{12}I_{26} + F_{12} - c_1H_{12}), \\ X_{110} &= -c_1(E_{11}I_{12} - E_{12}I_{21}), \\ X_{111} &= -c_1(2E_{66}I_{31} - E_{11}I_{11} + 2E_{12}I_{12} - E_{22}I_{21}), \\ X_{112} &= c_1(E_{12}I_{11} - E_{22}I_{12}), \\ X_{21} &= -A_{44} + 6c_1D_{44} - 9c_1^2F_{44}, \\ X_{22} &= -c_1(B_{11}I_{15} + F_{11} + B_{12}I_{25} - c_1E_{11}I_{15} - c_1H_{11} - c_1E_{12}I_{25}), \\ X_{23} &= -c_1(B_{11}I_{16} + B_{12}I_{26} + F_{12} + 2B_{66}I_{33} + 2F_{66} \\ &- 2c_1E_{66}I_{33} - 2c_1H_{66} - c_1E_{11}I_{16} - c_1E_{12}I_{26} - c_1H_{12}), \\ X_{24} &= B_{11}I_{13} - c_1B_{11}I_{15} + D_{11} - c_1F_{11} + B_{12}I_{23} - c_1B_{12}I_{25} \\ &- c_1E_{11}I_{13} + c_1^2E_{11}I_{15} - c_1F_{11} + c_1^2H_{11} \\ &- c_1E_{12}I_{23} + c_1^2E_{12}I_{25}, X_{25} = B_{66}I_{32} - c_1B_{66}I_{33} + D_{66} \\ &- c_1F_{66} - c_1E_{66}I_{32} + c_1^2E_{66}I_{33} - c_1F_{66} + c_1^2H_{66}, \\ X_{26} &= B_{11}I_{14} - c_1B_{11}I_{16} + B_{12}I_{24} - c_1B_{12}I_{26} + D_{12} - c_1F_{12} \\ &+ B_{66}I_{32} - c_1B_{66}I_{33} + D_{66} - c_1F_{66} - c_1E_{66}I_{32} \\ &+ c_1^2E_{66}I_{33} - c_1F_{66} + c_1^2H_{66} - c_1E_{11}I_{14} + c_1^2E_{11}I_{16} \\ &- c_1E_{12}I_{24} + c_1^2E_{12}I_{26} - c_1F_{12} + c_1^2H_{12}, \\ X_{27} &= -B_{11}I_{12} + B_{12}I_{21} + c_1E_{11}I_{12} - c_1E_{12}I_{21}, \\ X_{28} &= B_{11}I_{11} - B_{12}I_{12} - B_{66}I_{31} - c_1E_{11}I_{11} + c_1E_{12}I_{12} \\ &+ c_1E_{66}I_{31}, X_{31} = -A_{55} + 6c_1D_{55} - 9c_1^2F_{55}, \\ X_{32} &= -c_1(2B_{66}I_{33} + 2F_{66} + B_{12}I_{15} + F_{12} + B_{22}I_{25} \\ &- 2c_1E_{66}I_{33} - 2c_1H_{66} - c_1E_{12}I_{15} - c_1H_{12} - c_1E_{22}I_{25}), \\ X_{33} &= -c_1(B_{12}I_{16} + B_{22}I_{26} + F_{22} - c_1E_{12}I_{16} - c_1E_{22}I_{26} - c_1H_{22}), \\ X_{34} &= B_{66}I_{32} - c_1B_{66}I_{33} + D_{66} - c_1F_{66} + B_{12}I_{13} \\ &- c_1B_{12}I_{15} + D_{12} - c_1F_{12} + B_{22}I_{23} - c_1B_{22}I_{25} - c_1E_{66}I_{32} \\ &+ c_1^2E_{66}I_{33} - c_1F_{66} + c_1^2H_{66} - c_1E_{12}I_{13} + c_1^2E_{12}I_{15} \\ &- c_1F_{12} + c_1^2H_{12} - c_1E_{22}I_{23} + c_1^2E_{22}I_{25}, \\ X_{35} &= B_{66}I_{32} - c_1B_{66}I_{33} + D_{66} - c_1F_{66} - c_1E_{66}I_{32} \\ &+ c_1^2E_{66}I_{33} - c_1F_{66} + c_1^2H_{66},\end{aligned}$$

$$\begin{aligned}
 X_{36} &= B_{12}I_{14} - c_1B_{12}I_{16} + B_{22}I_{24} - c_1B_{22}I_{26} + D_{22} \\
 &\quad - c_1F_{22} - c_1E_{12}I_{14} + c_1^2E_{12}I_{16} - c_1E_{22}I_{24} \\
 &\quad + c_1^2E_{22}I_{26} - c_1F_{22} + c_1^2H_{22}, \\
 X_{37} &= -B_{66}I_{31} - B_{12}I_{12} + B_{22}I_{21} \\
 &\quad + c_1E_{66}I_{31} + c_1E_{12}I_{12} - c_1E_{22}I_{21}, \\
 X_{38} &= B_{12}I_{11} - B_{22}I_{12} - c_1E_{12}I_{11} + c_1E_{22}I_{12}.
 \end{aligned}$$

Appendix D

$$\begin{aligned}
 J_1 &= I_{31} - 2I_{12}, \quad J_2 = I_{23} - c_1I_{25}, \\
 J_3 &= I_{13} - c_1I_{15} - I_{32} + c_1I_{33}, \\
 J_4 &= I_{14} - c_1I_{16}, \quad J_5 = I_{24} - c_1I_{26} - I_{32} \\
 &\quad + c_1I_{33}, \quad J_6 = -c_1I_{15} - c_1I_{26} + 2c_1I_{33}.
 \end{aligned}$$

Appendix E

$$\begin{aligned}
 r_{11} &= -k_1 - k_2(\lambda_m^2 + \delta_n^2) + X_{13}\lambda_m^4 + X_{14}\lambda_m^2\delta_n^2 \\
 &\quad + X_{15}\delta_n^4 + X_{110}Q_1\lambda_m^4 + X_{111}Q_1\lambda_m^2\delta_n^2 + X_{112}Q_1\delta_n^4 \\
 &\quad - Q_1\frac{\lambda_m^2}{R}, \quad r_{12} = -X_{11}\lambda_m + X_{16}\lambda_m^3 + X_{17}\lambda_m\delta_n^2 \\
 &\quad + X_{110}Q_2\lambda_m^4 + X_{111}Q_2\lambda_m^2\delta_n^2 + X_{112}Q_2\delta_n^4 \\
 &\quad - Q_2\frac{\lambda_m^2}{R}, \quad r_{13} = -X_{12}\delta_n + X_{18}\delta_n^3 + X_{19}\lambda_m^2\delta_n \\
 &\quad + X_{110}Q_3\lambda_m^4 + X_{111}Q_3\lambda_m^2\delta_n^2 + X_{112}Q_3\delta_n^4 \\
 &\quad - Q_3\frac{\lambda_m^2}{R}, \quad r_{14} = \frac{32Q_2\lambda_m\delta_n}{3LR\pi}, \quad r_{15} = \frac{32Q_3\lambda_m\delta_n}{3LR\pi}, \\
 n_1 &= -X_{11}\lambda_m^2 - X_{12}\delta_n^2, \quad n_2 = \frac{32Q_1\lambda_m\delta_n}{3LR\pi},
 \end{aligned}$$

$$\begin{aligned}
 n_3 &= \frac{2\delta_n}{3LR\pi I_{21}\lambda_m R} - \frac{8X_{110}\lambda_m\delta_n}{3LR\pi I_{21}} - \frac{8X_{112}\lambda_m\delta_n}{3LR\pi I_{11}}, \\
 n_4 &= -\frac{\lambda_m^4}{16I_{11}} - \frac{\delta_n^4}{16I_{21}}, \quad n_5 = \frac{16}{mn\pi^2}, \\
 r_{21} &= -\lambda_m^3(X_{22} + Q_1X_{27}) - \lambda_m\delta_n^2(X_{23} + Q_1X_{28}), \\
 r_{22} &= X_{21} - X_{24}\lambda_m^2 - X_{25}\delta_n^2 - X_{27}Q_2\lambda_m^3 \\
 &\quad - X_{28}Q_2\lambda_m\delta_n^2, \\
 r_{23} &= -X_{26}\lambda_m\delta_n - X_{27}Q_3\lambda_m^3 - X_{28}Q_3\lambda_m\delta_n^2, \\
 n_6 &= X_{21}\lambda_m, \quad n_7 = \frac{8X_{27}\delta_n}{3LR\pi I_{21}}, \\
 r_{31} &= -\delta_n^3(X_{33} + Q_1X_{38}) - \lambda_m^2\delta_n(X_{32} + Q_1X_{37}), \\
 r_{32} &= -X_{34}\lambda_m\delta_n - X_{38}Q_2\delta_n^3 - D_{37}Q_2\lambda_m^2\delta_n, \\
 r_{33} &= X_{31} - X_{35}\lambda_m^2 - X_{36}\delta_n^2 - X_{38}Q_3\delta_n^3 \\
 &\quad - X_{37}Q_3\lambda_m^2\delta_n, \quad n_8 = X_{31}\delta_n, \quad n_9 = \frac{8X_{38}\lambda_m}{3LR\pi I_{11}}.
 \end{aligned}$$

References

Ahmed, M.K.: Buckling behavior of a radially loaded corrugated orthotropic thin-elliptic cylindrical shell on an elastic foundation. *Thin Walled Struct.* **107**, 90–100 (2016)

Alibeigloo, A.: Free vibration analysis of functionally graded carbon nanotube-reinforced composite cylindrical panel embedded in piezoelectric layers by using theory of elasticity. *Eur. J. Mech. A Solids* **44**, 104–115 (2014)

Arani, A.G., Haghparast, E., Khoddami Maraghi, Z., Amir, S.: CNTRC cylinder under non-axisymmetric thermo-mechanical loads and uniform electromagnetic fields. *Arab. J. Sci. Eng.* **39**, 9057–9069 (2014)

Asadi, H., Wang, Q.: Dynamic stability analysis of a pressurized FG-CNTRC cylindrical shell interacting with supersonic airflow. *Compos. B Eng.* **118**, 15–25 (2017)

Baloch, W.L., Khushnood, R.A., Khaliq, W.: Influence of multi-walled carbon nanotubes on the residual performance of concrete exposed to high temperatures. *Constr. Build. Mater.* **185**, 44–56 (2018)

Brush, D.D., Almroth, B.O.: *Buckling of bars, plates and shells.* McGraw-Hill, New York (1975)

Chen, Y., Jin, G., Zhang, C., Ye, T., Xue, Y.: Thermal vibration of FGM beams with general boundary conditions using a higher-order shear deformation theory. *Compos. B Eng.* **153**, 376–386 (2018)

Dastjerdi, S., Abbasi, M., Yazdanparast, L.: A new modified higher-order shear deformation theory for nonlinear analysis of macro- and nano-annular sector plates using the extended Kantorovich method in conjunction with SAPM. *Acta Mech.* **228**, 3381–3401 (2017)

Duc, N.D., Quan, T.Q., Luat, V.D.: Nonlinear dynamic analysis and vibration of shear deformable piezoelectric FGM

- double curved shallow shells under damping-thermo-electro-mechanical loads. *Compos. Struct.* **125**, 29–40 (2015)
- Duc, N.D., Tuan, N.D., Tran, P., Cong, P.H., Nguyen, P.D.: Nonlinear stability of eccentrically stiffened S-FGM elliptical cylindrical shells in thermal environment. *Thin Walled Struct.* **108**, 280–290 (2016)
- Duc, N.D., Quan, T.Q., Khoa, N.D.: New approach to investigate nonlinear dynamic response and vibration of imperfect functionally graded carbon nanotube reinforced composite double curved shallow shells subjected to blast load and temperature. *Aerosp. Sci. Technol.* **71**, 360–372 (2017)
- Ganapathi, M., Patel, B.P., Patel, H.G.: Free flexural vibration behavior of laminated angle-ply elliptical cylindrical shells. *Comput. Struct.* **82**, 509–518 (2004)
- Jadhav, P., Bajoria, K.: Stability analysis of thick piezoelectric metal based FGM plate using first order and higher order shear deformation theory. *Int. J. Mech. Mater. Des.* **11**, 387–403 (2015)
- Kazemi, E., Darvizeh, M., Darvizeh, A., Ansari, R.: An investigation of the buckling behavior of composite elliptical cylindrical shells with piezoelectric layers. *Acta Mech.* **223**, 2225–2242 (2012)
- Keleshteri, M.M., Asadi, H., Wang, Q.: Postbuckling analysis of smart FG-CNTRC annular sector plates with surface-bonded piezoelectric layers using generalized differential quadrature method. *Comput. Methods Appl. Mech. Eng.* **325**, 689–710 (2017)
- Khalifa, M.: Effects of non-uniform Winkler foundation and non-homogeneity on the free vibration of an orthotropic elliptical cylindrical shell. *Eur. J. Mech. A Solids* **49**, 570–581 (2015)
- Kumar, R.S., Kundalwal, S.I., Ray, M.C.: Control of large amplitude vibrations of doubly curved sandwich shells composed of fuzzy fiber reinforced composite facings. *Aerosp. Sci. Technol.* **70**, 10–28 (2017)
- Kundalwal, S.I., Meguid, S.A.: Effect of carbon nanotube waviness on active damping of laminated hybrid composite shells. *Acta Mech.* **226**, 2035–2052 (2015)
- Kundalwal, S.I., Ray, M.C.: Smart damping of fuzzy fiber reinforced composite plates using 1–3 piezoelectric composites. *J. Vib. Control* **22**, 1526–1546 (2016)
- Lam, K.Y., Loy, C.T.: Effects of boundary conditions on frequencies of a multilayered cylindrical shell. *J. Sound Vib.* **188**, 363–384 (1995)
- Lei, Z.X., Zhang, L.W., Liew, K.M.: Buckling analysis of CNT reinforced functionally graded laminated composite plates. *Compos. Struct.* **152**, 62–73 (2016)
- Li, T.Y., Xiong, L., Zhu, X., Xiong, Y.P., Zhang, G.J.: The prediction of the elastic critical load of submerged elliptical cylindrical shell based on the vibro-acoustic model. *Thin Walled Struct.* **84**, 255–262 (2014)
- Mantari, J.L., Oktem, A.S., Guedes Soares, C.: Bending and free vibration analysis of isotropic and multilayered plates and shells by using a new accurate higher-order shear deformation theory. *Compos. B Eng.* **43**, 3348–3360 (2012)
- Mirzaei, M., Kiani, Y.: Thermal buckling of temperature dependent FG-CNT reinforced composite plates. *Meccanica* **51**, 2185–2201 (2016)
- Phung-Van, P., De Lorenzis, L., Thai, C.H., Abdel-Wahab, M., Nguyen-Xuan, H.: Analysis of laminated composite plates integrated with piezoelectric sensors and actuators using higher-order shear deformation theory and isogeometric finite elements. *Comput. Mater. Sci.* **96**, 495–505 (2015)
- Pradyumna, S., Bandyopadhyay, J.N.: Dynamic instability behavior of laminated hyper and conoid shells using a higher-order shear deformation theory. *Thin Walled Struct.* **49**, 77–84 (2011)
- Reddy, J.N.: *Mechanics of laminated composite plates and shells: theory and analysis*. CRC Press, Boca Raton (2004)
- Shen, H.S.: Nonlinear bending of functionally graded carbon nanotube-reinforced composite plates in thermal environments. *Compos. Struct.* **91**, 9–19 (2009)
- Shen, H.S.: Nonlinear vibration of shear deformable FGM cylindrical shells surrounded by an elastic medium. *Compos. Struct.* **94**, 1144–1154 (2012)
- Shen, H.-S., Xiang, Y.: Nonlinear vibration of nanotube-reinforced composite cylindrical shells in thermal environments. *Comput. Methods Appl. Mech. Eng.* **213–216**, 196–205 (2012)
- Tu, T.M., Thach, L.N., Quoc, T.H.: Finite element modeling for bending and vibration analysis of laminated and sandwich composite plates based on higher-order theory. *Comput. Mater. Sci.* **49**, S390–S394 (2010)
- Xie, F., Qu, Y., Zhang, W., Peng, Z., Meng, G.: Nonlinear thermoelastic analysis of composite laminated panels using a general higher-order shear deformation zig-zag theory. *Int. J. Mech. Sci.* **150**, 226–237 (2019)
- Xu, Z., Gardner, L., Sadowski, A.J.: Nonlinear stability of elastic elliptical cylindrical shells under uniform bending. *Int. J. Mech. Sci.* **128–129**, 593–606 (2017)
- Xuebin, L.: Study on free vibration analysis of circular cylindrical shells using wave propagation. *J. Sound Vib.* **311**, 667–682 (2008)
- Zarei, H., Fallah, M., Bisadi, H., Daneshmehr, A.R., Minak, G.: Multiple impact response of temperature-dependent carbon nanotube-reinforced composite (CNTRC) plates with general boundary conditions. *Compos. B Eng.* **113**, 206–217 (2017)
- Zhang, G.J., Li, T.Y., Zhu, X., Yang, J., Miao, Y.Y.: Free and forced vibration characteristics of submerged finite elliptical cylindrical shell. *Ocean Eng.* **129**, 92–106 (2017)

Publisher's Note Springer Nature remains neutral with regard to jurisdictional claims in published maps and institutional affiliations.